10. Arai, S., Miyake, K., Voit, R., Nemoto, S., Wakeland, E. K., Grummt, I., and Miyazaki, T. (2007) *Proc. Natl. Acad. Sci. U. S. A.* **104,** 2289–2294
11. Miyazaki, T., and Arai, S. (2007) *Cell Cycle* **6,** 1419–1425
12. Stegh, A. H., Schickling, O., Ehret, A., Scaffidi, C., Peterhänsel, C., Hofmann, T. G., Grummt, I., Krammer, P. H., and Peter, M. E. (1998) *EMBO J.* **17,** 5974–5986
13. Oldham, S., and Hafen, E. (2003) *Trends Cell Biol.* **13,** 79–85
14. Valentinis, B., and Baserga, R. (2001) *Mol. Pathol.* **54,** 133–137
15. Vogt, P. K. (2001) *Trends Mol. Med.* **7,** 482–484
16. Huang, S., and Houghton, P. J. (2003) *Curr. Opin. Pharmacol.* **3,** 371–377
17. Shamji, A. F., Nghiem, P., and Schreiber, S. L. (2003) *Mol. Cell* **12,** 271–280
18. Fingar, D. C., Salama, S., Tsou, C., Harlow, E., and Blenis, J. (2002) *Genes Dev.* **16,** 1472–1487
19. Shima, H., Pende, M., Chen, Y., Fumagalli, S., Thomas, G., and Kozma, S. C. (1998) *EMBO J.* **17,** 6649–6659
20. Montagne, J., Stewart, M. J., Stocker, H., Hafen, E., Kozma, S. C., and Thomas, G. (1999) *Science* **285,** 2126–2129
21. Pende, M., Kozma, S. C., Jaquet, M., Oorschot, V., Burcelin, R., Le Marchand-Brustel, Y., Klumperman, J., Thorens, B., and Thomas, G. (2000) *Nature* **408,** 994–997
22. Fingar, D. C., and Blenis, J. (2004) *Oncogene* **23,** 3151–3171
23. Ohanna, M., Sobering, A. K., Lapointe, T., Lorenzo, L., Praud, C., Petroulakis, E., Sonenberg, N., Kelly, P. A., Sotiropoulos, A., and Pende, M. (2005) *Nat. Cell Biol.* **7,** 286–294
24. Um, S. H., D'Alessio, D., and Thomas, G. (2006) *Cell Metab.* **3,** 393–402
25. Dann, S. G., Selvaraj, A., and Thomas, G. (2007) *Trends Mol. Med.* **13,** 252–259
26. Pullen, N., and Thomas, G. (1997) *FEBS Lett.* **410,** 78–82
27. Papst, P. J., Sugiyama, H., Nagasawa, M., Lucas, J. J., Maller, J. L., and Terada, N. (1998) *J. Biol. Chem.* **273,** 15077–15084
28. Shah, O. J., Ghosh, S., and Hunter, T. (2003) *J. Biol. Chem.* **278,** 16433–16442
29. Schmidt, T., Wahl, P., Wüthrich, R. P., Vogetseder, A., Picard, N., Kaissling, B., and Le Hir, M. (2007) *Histochem. Cell Biol.* **127,** 123–129
30. Hou, Z., He, L., and Qi, R. Z. (2007) *J. Biol. Chem.* **282,** 6922–6928
31. Boyer, D., Quintanilla, R., and Lee-Fruman, K. K. (2007) *Mol. Cell. Biochem.* **307,** 59–64
32. Kubota, N., Tobe, K., Terauchi, Y., Eto, K., Yamauchi, T., Suzuki, R., Tsubamoto, Y., Komeda, K., Nakano, R., Miki, H., Satoh, S., Sekihara, H., Sciacchitano, S., Lesniak, M., Aizawa, S., Nagai, R., Kimura, S., Akanuma, Y., Taylor, S. I., and Kadowaki, T. (2000) *Diabetes* **49,** 1880–1889
33. McMullen, J. R., Shioi, T., Zhang, L., Tarnavski, O., Sherwood, M. C., Dorfman, A. L., Longnus, S., Pende, M., Martin, K. A., Blenis, J., Thomas, G., and Izumo, S. (2004) *Mol. Cell. Biol.* **24,** 6231–6240
34. Miyazaki, J., Araki, K., Yamato, E., Ikegami, H., Asano, T., Shibasaki, Y., Oka, Y., and Yamamura, K. (1990) *Endocrinology* **127,** 126–132
35. Tibbetts, M. D., Zheng, L., and Lenardo, M. J. (2003) *Nat. Immunol.* **4,** 404–409
36. Gudur Valmiki, M., and Ramos, J. W. *Cell. Mol. Life Sci.*, in press
37. Arechiga, A. F., Bell, B. D., Leverrier, S., Weist, B. M., Porter, M., Wu, Z., Kanno, Y., Ramos, S. J., Ong, S. T., Siegel, R., and Walsh, C. M. (2007) *J. Immunol.* **179,** 5291–5300
38. Park, S., Ramnarain, D. B., Hatanpaa, K. J., Mickey, B. E., Saha, D., Paulmurugan, R., Madden, C. J., Wright, P. S., Bhai, S., Ali, M. A., Puttaparthi, K., Hu, W., Elliott, J. L., Stuve, O., and Habib, A. A. (2008) *EMBO Rep.* **9,** 766–773
39. Schumann, D. M., Maedler, K., Franklin, I., Konrad, D., Størling, J., Böni-Schnetzler, M., Gjinovci, A., Kurrer, M. O., Gauthier, B. R., Bosco, D., Andres, A., Berney, T., Greter, M., Becher, B., Chervonsky, A. V., Halban, P. A., Mandrup-Poulsen, T., Wollheim, C. B., and Donath, M. Y. (2007) *Proc. Natl. Acad. Sci. U. S. A.* **104,** 2861–2866
40. Pearson, R. B., Dennis, P. B., Han, J. W., Williamson, N. A., Kozma, S. C., Wettenhall, R. E., and Thomas, G. (1995) *EMBO J.* **14,** 5279–5287
41. Yang, Q., Inoki, K., Kim, E., and Guan, K. L. (2006) *Proc. Natl. Acad. Sci. U. S. A.* **103,** 6811–6816

The FASEB Journal • Research Communication

Neuronal IGF-1 resistance reduces Aβ accumulation and protects against premature death in a model of Alzheimer's disease

Susanna Freude,[*,†,‡,1] Moritz M. Hettich,[*,†,‡,1] Christina Schumann,[*,†] Oliver Stöhr,[*,†,‡] Linda Koch,[†,‡,§] Christoph Köhler,[‖] Michael Udelhoven,[*,†,‡] Uschi Leeser,[*,†,‡] Marita Müller,[*,†,‡] Naoto Kubota,[¶] Takashi Kadowaki,[¶] Wilhelm Krone,[*,†,‡] Hannsjörg Schröder,[‖] Jens C. Brüning,[*,†,‡,§,#] and Markus Schubert[*,†,‡,2]

[*]Department of Internal Medicine II, [†]Center for Molecular Medicine Cologne (CMMC), [‡]Cologne Excellence Cluster on Cellular Stress Responses in Aging-Associated Diseases (CECAD), [§]Department of Mouse Genetics and Metabolism, Institute for Genetics, and [‖]Department II of Anatomy, University of Cologne, Cologne, Germany; [¶]Department of Metabolic Diseases, Graduate School of Medicine, University of Tokyo, Tokyo, Japan; and [#]Max Planck Institute for the Biology of Ageing, Cologne, Germany

ABSTRACT **Alzheimer's disease (AD) is characterized by progressive neurodegeneration leading to loss of cognitive abilities and ultimately to death. Postmortem investigations revealed decreased expression of cerebral insulin-like growth factor (IGF)-1 receptor (IGF-1R) and insulin receptor substrate (IRS) proteins in patients with AD. To elucidate the role of insulin/IGF-1 signaling in AD, we crossed mice expressing the Swedish mutation of amyloid precursor protein (APP^{SW}, Tg2576 mice) as a model for AD with mice deficient for either IRS-2, neuronal IGF-1R (nIGF-$1R^{-/-}$), or neuronal insulin receptor (n$IR^{-/-}$), and analyzed survival, glucose, and APP metabolism. In the present study, we show that IRS-2 deficiency in Tg2576 mice completely reverses premature mortality in Tg2576 females and delays β-amyloid (Aβ) accumulation. Analysis of APP metabolism suggested that delayed Aβ accumulation resulted from decreased APP processing. To delineate the upstream signal responsible for IRS-2-mediated disease protection, we analyzed mice with nIGF-1R or nIR deficiency predominantly in the hippocampus. Interestingly, both male and female nIGF-$1R^{-/-}$Tg2576 mice were protected from premature death in the presence of decreased Aβ accumulation specifically in the hippocampus formation. However, neuronal IR deletion had no influence on lethality of Tg2576 mice. Thus, impaired IGF-1/IRS-2 signaling prevents premature death and delays amyloid accumulation in a model of AD.—Freude, S., Hettich, M. M., Schumann, C., Stöhr, O., Koch, L., Köhler, C., Udelhoven, M., Leeser, U., Müller, M., Kubota, N., Kadowaki, T., Krone, W., Schröder, H., Brüning, J. C., Schubert, M. Neuronal IGF-1 resistance reduces Aβ accumulation and protects against premature death in a model of Alzheimer's disease. *FASEB J.* 23, 3315–3324 (2009). www.fasebj.org**

Key Words: β-amyloid · longevity · insulin receptor substrate · brain · Tg2576 mice

ALZHEIMER'S DISEASE (AD), the most common cause of dementia, is irreversible, and patients become completely dependent on others even for the simplest of daily activities (1). Furthermore, AD is associated with a high mortality, especially in patients aged 65–74 yr, with a median survival of only 3.8 yr after initial diagnosis (2). Even though recent reports suggest that type 2 diabetes mellitus (T2DM) is a risk factor for AD (3–6), the underlying cellular mechanisms for this association are still unknown. It is conceivable that vascular complications of T2DM result in neurodegeneration (7). Alternatively, neuronal insulin/insulin-like growth factor-1 (IGF-1) resistance might represent the unifying link between T2DM and AD, characterizing AD as a "brain-type diabetes" (7–10). In agreement with this hypothesis is the observation that insulin receptor (IR) and insulin-like growth factor-1 receptor (IGF-1R) signaling is markedly disturbed in the central nervous system (CNS) of patients with AD (11–13). Postmortem investigations of brains from patients with AD revealed a substantially down-regulated expression of IR, IGF-1R, and insulin receptor substrate (IRS) proteins (8, 14), these changes progressing with severity of neurodegeneration. One common feature in neurons from patients with AD is down-regulation of IRS-2 and IGF-1R (8, 13). Other groups reported similar results in AD brains (13). These findings raise the important question, whether changes in IR/IGF-1R signaling (IIS) are cause, consequence, or maybe even compensatory counterregulation of neurodegeneration.

One major pathological hallmark of AD is accumulation of β-amyloid (Aβ) peptides, which are toxic and mainly occur in 2 lengths: $A\beta_{1\text{-}40}$ and $A\beta_{1\text{-}42}$. Aβ evolves from cleavage of amyloid precursor protein (APP) by specific secretases. In *Caenorhabditis elegans,* the DAF-2 pathway as ortholog of the mammalian IIS is proposed

[1] These authors contributed equally to this work.

[2] Correspondence: Department of Internal Medicine II, University of Cologne, Kerpener Str. 62, LFI 4/061, 50937 Cologne, Germany. E-mail: markus.schubert@uni-koeln.de

doi: 10.1096/fj.09-132043

to control longevity (15). Decreased DAF-2 signaling causes up to a 3-fold lifespan extension (16–18). It has been shown that knocking down DAF-2 in *C. elegans* reduces $A\beta_{1-42}$ toxicity (19), which has led to the proposal that the DAF-2 pathway controls detoxification of $A\beta_{1-42}$ disassemblies. Taken together, these data suggest a major role for IIS in detoxification of Aβ, thereby influencing survival of patients with AD. To further analyze the role of IIS in the pathogenesis of AD, we created mice expressing the Swedish mutation of APP_{695} (Tg2576 mice) deficient for IRS-2, neuronal IGF-1Rs, or neuronal IRs. In the present study, we show that specifically impaired IGF-1R/IRS-2 signaling protects from premature lethality of Tg2576 mice and reduces Aβ accumulation.

MATERIALS AND METHODS

Animals, breeding, and genotyping

IRS-$2^{-/-}$ mice were generated, maintained, and genotyped as described previously (20). Wild-type (WT) littermates were used as controls. Tg2576 mice with transgenic expression of the Swedish mutation of APP_{695} (APP^{SW}) in a B6/SJL background were purchased from Taconic (Hudson, NY, USA). Since the genetic background of Tg2576 mice might influence mortality (21), we used the APP^{SW} model in a B6/SJL background from Taconic and crossed these mice back for 3 generations in a C57BL/6 background. Because of this approach, we obtained in all 3 intercrossed strains (IRS-$2^{-/-}$, nIGF-$1R^{-/-}$, and $nIR^{-/-}$) similar mortality rates of Tg2576 mice as described in the literature (22–24). IGF-$1R^{lox/lox}$ and $IR^{lox/lox}$ mice were generated and genotyped as described previously (25, 26) and crossed with synapsin-Cre (Syn-Cre) mice to achieve neuron-specific deletion. Mice that did not express APP^{SW} or Syn-Cre served as controls. Animals were housed in a 12-h light-dark cycle (7 AM on, 7 PM off) and were fed a standard rodent diet (breeding diet 1314; Altromin, Lage, Germany: 89% dry matter, 22.5% crude protein, 5% crude fat, 4.5% crude fiber, 6.5% crude ash, 50.5% nitrogen-free extracts, and a standard amount of different minerals, amino acids, vitamins, and trace elements). All animal procedures were performed in accordance with the German Laws for Animal Protection and were approved by the local animal care committee and the Bezirksregierung Köln.

Histology and immunostaining

Syn-Cre mice were crossed with RosaArte1 reporter mice (27). Syn-Cre-LacZ mice were anesthetized and transcardially perfused with physiological saline solution, followed by 4% paraformaldehyde in 0.1 M PBS (pH 7.4). Brains were then frozen in tissue-freezing medium (Jung Tissue Freezing Medium; Leica Microsystems, Wetzlar, Germany) and sectioned on a cryostat. Staining of dissected tissues was performed using antibodies against β-galactosidase (55976; Cappel; MP Biomedicals, Santa Ana, CA, USA). Slides were viewed through a Zeiss Axioskop equipped with a Zeiss AxioCam for acquisition of digital images using Spot Advanced 3.0.3 software (Carl Zeiss, Oberkochen, Germany).

Immunoblotting

Brains were lysed in buffer (50 mM Hepes, pH 7.4; 50 mM NaCl; 1% Triton X; 10 mM EDTA; 0.1 M NaF; 17 μg/ml aprotinine; 2 mM benzanidine; 0.1% SDS; 1 mM phenylmethylsulfonyl fluoride; and 10 mM Na_3VO_4) using a polytron. Protein expression was determined from whole-brain lysates (50–100 μg) dissolved in Laemmli buffer and resolved on 7.5 or 15% SDS-PAGE gels. Proteins were transferred to PVDF, and membranes were blocked with 5% Western blot blocking solution and incubated with the appropriate antisera.

The following primary antibodies were used: insulin receptor β-subunit (IRβ), A disintegrin and metalloprotease-10 (ADAM-10) (Santa Cruz Biotechnology, Santa Cruz, CA, USA), actin (MP Biomedicals, Solon, OH, USA), β-site APP cleaving enzyme (BACE), Aβ, insulin degrading enzyme (IDE; Chemicon International/Upstate, Millipore, MA, USA), protein kinase B, phospho-PKB (AKT), extracellular regulated kinase (ERK)-1/2, phospho-ERK-1/2, glycogen synthase kinase (GSK)-3β, phospho-GSK-3β, APP, IGF-1R (Cell Signaling Technology Inc., Danvers, MA, USA), C-terminal fragments-α/β (CTF-α/β) (Sigma Aldrich, Munich, Germany), and 6E10 ($A\beta_{1-17}$; Covance, Princeton, NJ, USA). The secondary antibodies anti-mouse-IgG and anti-rabbit-IgG were purchased from Sigma-Aldrich.

Metabolic characterization and glucose- and insulin-tolerance tests

Mice were weighed weekly beginning at weaning in wk 3 until performance of glucose- and insulin-tolerance tests in wk 10 and 11. From wk 12, blood glucose and weight were measured every 4 wk.

For insulin-tolerance tests, animals were starved overnight (16 h) and injected with 0.75 U/kg body weight of human insulin (Novo Nordisk, Copenhagen, Denmark) into the peritoneal cavity. Blood glucose levels were measured in blood collected from the tail tip immediately before and 15, 30, and 60 min after injection. Blood glucose measurements were performed using a blood glucose meter (GlucoMen; A. Menarini Diagnostics, Berlin-Chemie, Neuss, Germany). Results were expressed as percentage of initial blood glucose concentration.

For glucose-tolerance tests, mice were starved overnight (16 h). Animals were injected with glucose (2 g/kg body weight) into the peritoneal cavity. Glucose levels were determined in blood collected from the tail tip immediately before and 15, 30, 60, and 120 min after the injection, using a glucose meter.

β-Secretase activity assay

Activity of β-secretase was measured following the manufacturers protocol at 535 nm emission (FP002; R&D Systems Inc., Minneapolis, MN, USA).

$A\beta_{1-40}$ and $A\beta_{1-42}$ ELISA

Amyloid was extracted using 5 M guanidine HCl in 50 mM Tris HCl, pH 8.0. Then ELISAs of $A\beta_{1-40}$ and $A\beta_{1-42}$ were performed following the manufacturer's protocol (KHB3481/3441; Invitrogen Corp., Carlsbad, CA, USA).

Statistical analysis

To quantify the changes in optical density, we used the software AIDA 4.00.027 (Raytest, Straubenhardt, Germany). For statistical analysis of the different study groups, unpaired Student's *t* test was performed. Statistical significance was defined as $P < 0.05$. For Kaplan-Meier analysis, XLSTAT-Life software, a Microsoft Excel add-in (http://www.xlstat.com),

was used. For comparison of the different study groups, Wilcoxon rank tests were performed. Statistical significance was defined as $P < 0.05$.

RESULTS

IRS-2 deficiency rescues APP^{SW}-induced mortality in mice

To directly address the importance of IGF-1R/IRS-2 signaling in the pathogenesis of AD, we first crossed IRS-2-deficient (IRS-$2^{-/-}$) mice with mice expressing the Swedish mutation of human APP_{695} containing the double mutation $Lys^{670} \rightarrow Asn$, $Met^{671} \rightarrow Leu$, which was found in a Swedish family with early-onset AD (APP^{SW}, Tg2576 mice) (28). Tg2576 mice display an age-dependent memory impairment, increase of Aβ levels starting at 2 mo of age, and extracellular plaque formation beginning at the age of 8 mo (29). Since brain-specific IRS-2 deficiency as well as body-wide heterozygous IRS-2 deletion increase longevity (at least in some studies; see refs. 30, 31), we investigated the influence of IRS-2 deficiency on APP^{SW}-induced mortality. Strikingly, IRS-2 deficiency reverses the premature lethality of female Tg2576 mice completely (23, 32) (**Fig. 1*A***). In males, lack of IRS-2 does not rescue mortality of Tg2576 mice. Since male IRS-$2^{-/-}$ mice frequently develop hyperglycemia (33) (Fig. 1*B*) and impaired glucose tolerance (Fig. 1*C*), overt hyperglycemia might affect mortality in these mice. To further analyze a potential role of hyperglycemia in viability of Tg2576 males, we classified IRS-$2^{-/-}$Tg2576 mice according to the presence or absence of hyperglycemia, defined as 2 or more events of blood glucose levels >2 SD above age-matched control mice (Fig. 1*E* and Supplemental Fig. 1*A*). All hyperglycemic IRS-$2^{-/-}$Tg2576 males die before the age of 32 wk, while euglycemic IRS-$2^{-/-}$Tg2576 males survive (Supplemental Fig. 1*A*). Moreover, IRS-2 deficiency in euglycemic male Tg2576 mice rescues premature death of Tg2576 males (Supplemental Fig. 1*B*). This effect is specific for the Tg2576 background, because hyperglycemic IRS-$2^{-/-}$ males do not show increased mortality compared to euglycemic male IRS-$2^{-/-}$ mice up to 48 wk of age (data not shown). Blood glucose levels of IRS-$2^{-/-}$Tg2576 males dying prematurely are significantly higher compared to surviving IRS-$2^{-/-}$Tg2576 males (Supplemental Fig. 1*B*), reinforcing the role of hyperglycemia on survival of Tg2576 mice. However, differences in body weight and growth did not account for the observed differences in survival (Fig. 1*D*).

IRS-2 alters IR/IGF-1R signaling and APP processing

Consistent with a major role for IRS-2 in cerebral IR/IGF-1 signaling, we observed significantly reduced phosphorylation of proteins in PI3-kinase and MAP kinase pathway, namely, GSK-3β and ERK-1/2, as well as a slight reduction in phosphorylation of PKB (AKT) in 12-wk-old IRS-$2^{-/-}$ brains compared to WT under steady-state conditions (**Fig. 2*A***). However, there was no reduction in phosphorylation of ERK-1/2 and GSK-3β detectable in brain lysates from Tg2576 compared to WT and IRS-$2^{-/-}$Tg2576 mice. Previous studies suggest that increased IGF-2 expression might partially rescue states of insulin resistance in Tg2576 mice, which might possibly explain the difference in ERK and GSK-3β phosphorylation between IRS-$2^{-/-}$ and IRS-$2^{-/-}$Tg2576 mice (29).

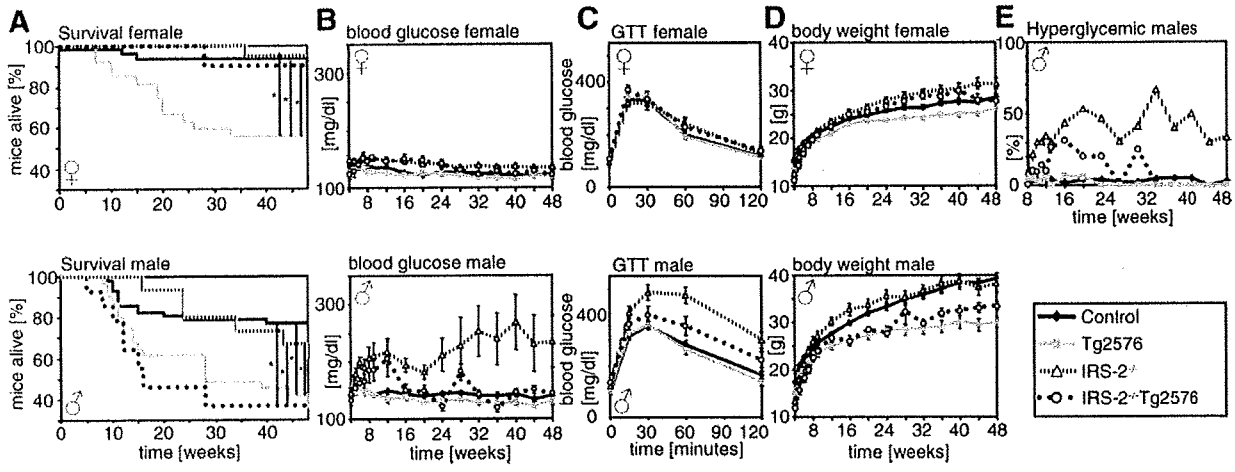

Figure 1. Kaplan-Meier analysis and metabolic characterization of IRS-$2^{-/-}$Tg2576 mice and respective controls up to the age of 48 wk. *A*) Kaplan-Meier analysis. Survival was assessed from 101 female (43 WT, 27 Tg2576, 21 IRS-$2^{-/-}$, 10 IRS-$2^{-/-}$Tg2576) and 117 male mice (57 WT, 31 Tg2576, 15 IRS-$2^{-/-}$, 14 IRS-$2^{-/-}$Tg2576). *$P < 0.05$; Wilcoxon rank test. *B*) Blood glucose levels. Blood glucose levels were assessed from 173 female (72 WT, 48 Tg2576, 33 IRS-$2^{-/-}$, 20 IRS-$2^{-/-}$Tg2576) and 165 male mice (79 WT, 43 Tg2576, 23 IRS-$2^{-/-}$, 20 IRS-$2^{-/-}$Tg2576). *C*) Glucose-tolerance tests (GTT) of mice aged 10–11 wk. Glucose tolerance was assessed from 156 female (64 WT, 39 Tg2576, 33 IRS-$2^{-/-}$, 20 IRS-$2^{-/-}$Tg2576) and 146 male mice (66 WT, 37 Tg2576, 23 IRS-$2^{-/-}$, 20 IRS-$2^{-/-}$Tg2576). *D*) Body weight. Body weight was assessed from 173 female (72 WT, 48 Tg2576, 33 IRS-$2^{-/-}$, 20 IRS-$2^{-/-}$Tg2576) and 165 male mice (79 WT, 43 Tg2576, 23 IRS-$2^{-/-}$, 20 IRS-$2^{-/-}$Tg2576). *E*) Male mice with hyperglycemia, defined as 2 or more events of blood glucose >2 SD above age-matched control mice. Data represent percentage of animals with blood glucose levels > mean blood $glucose_{control}$ + 2 SD. Data are expressed as means ± SE.

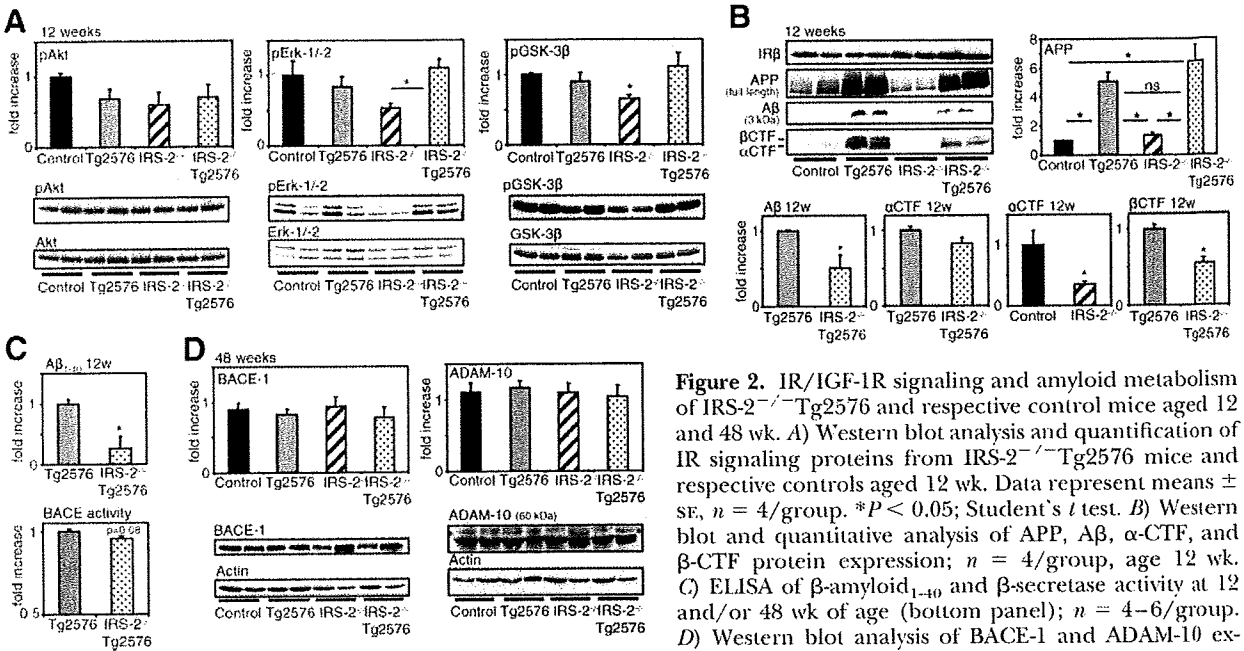

Figure 2. IR/IGF-1R signaling and amyloid metabolism of IRS-2$^{-/-}$Tg2576 and respective control mice aged 12 and 48 wk. *A*) Western blot analysis and quantification of IR signaling proteins from IRS-2$^{-/-}$Tg2576 mice and respective controls aged 12 wk. Data represent means ± SE, $n = 4$/group. *$P < 0.05$; Student's t test. *B*) Western blot and quantitative analysis of APP, Aβ, α-CTF, and β-CTF protein expression; $n = 4$/group, age 12 wk. *C*) ELISA of β-amyloid$_{1-40}$ and β-secretase activity at 12 and/or 48 wk of age (bottom panel); $n = 4-6$/group. *D*) Western blot analysis of BACE-1 and ADAM-10 expression; $n = 4-6$/group, age 48 wk. Data represent means ± SE. *$P < 0.05$; Student's t test. Age-matched WT animals served as controls.

Since increased Aβ accumulation in the CNS might be a contributing factor of premature lethality in Tg2576 mice, we next investigated Aβ accumulation (23, 32). Aβ peptides are proteolytically released from the APP *via* sequential cleavage by two aspartyl proteases, the β- and γ-secretase, and cleavage products mainly occur in two lengths, Aβ$_{1-40}$ and Aβ$_{1-42}$. To investigate whether APP or APP cleavage products are affected in IRS-2$^{-/-}$Tg2576 mice, we performed Western blot analysis, revealing comparable cerebral transgenic APP levels in Tg2576 and IRS-2$^{-/-}$Tg2576 mice aged 12 wk (Fig. 2*B*). Interestingly, brains of 12-wk-old IRS-2$^{-/-}$Tg2576 mice showed significantly ($P<0.05$) less Aβ accumulation compared to Tg2576 mice (Fig. 2*B*). These findings were further confirmed by ELISA analysis detecting Aβ$_{1-40}$ (Fig. 2*C*), revealing a significant decrease of Aβ$_{1-40}$ peptides in brains from IRS-2$^{-/-}$ Tg2576 compared to Tg2576 mice at 12 wk. Since the reduced Aβ accumulation at 12 wk is present in both genders, these data indicate that insulin/IGF-1 resistance prevents Aβ accumulation, while organismal hyperglycemia, as present in male IRS-2-deficient mice, may counteract this beneficial effect with respect to APP^{SW}-induced mortality.

Since it has been previously demonstrated that IGF-1R-mediated signals increase α- and β-cleavage of APP (34, 35) in cultured cells, we next determined the abundance of β-CTF and α-CTF in the CNS of control and IRS-2-deficient mice (Fig. 2*B*). Interestingly, β-CTFs were significantly reduced in IRS-2$^{-/-}$Tg2576 compared to Tg2576 mice, while APP levels were unchanged. Furthermore, α-CTFs occur at lower levels in brains of IRS-2$^{-/-}$ as compared to WT mice and showed a slight reduction in IRS-2$^{-/-}$Tg2576 compared to Tg2576 mice (Fig. 2*B*). These data indicate that reduced Aβ accumulation observed in IRS-2$^{-/-}$Tg2576 mice results from decreased APP processing (Fig. 2*B*).

To analyze whether reduced expression of the different secretases accounts for altered APP cleavage in IRS-2$^{-/-}$Tg2576 mice, we investigated protein levels of the membrane-anchored aspartyl protease BACE-1, which acts as a β-secretase (Fig. 2*D*), and the disintegrin metalloprotease ADAM-10, proposed to act as α-secretase (Fig. 2*D*). There were no differences between the genotypes, which suggests that IRS-2 regulates α- and β-secretase processing independently of BACE-1 and ADAM-10 expression (Fig. 2*D*). Analysis of β-secretase activity revealed a slightly but not significantly reduced activity in IRS-2$^{-/-}$Tg2576 compared to Tg2576 mice (Fig. 2*C*). In light of the recent notion that already marginal reductions of β-secretase activity profoundly affect APP cleavage and disease progression (36), this mild reduction present in IRS-2-deficient mice may partially account for the observed delay in Aβ accumulation in these animals, or another so far unknown mechanism may be involved.

Similar to IRS-2$^{-/-}$Tg2576 mice aged 12 wk, these mice at age 48 wk also showed unaltered protein expression of IR and IGF-1R (**Fig. 3*A*, *B***). However, Western blot analysis (Fig. 3*C*) and ELISAs (Fig. 3*D*) of Aβ$_{1-40}$ and Aβ$_{1-42}$ expression at 48 wk of age revealed no difference in total Aβ accumulation between IRS-2$^{-/-}$ Tg2576 and Tg2576 mice, indicating that Aβ accumulation is delayed but not abolished in IRS-2$^{-/-}$Tg2576 animals. BACE activity as well as BACE-1 protein expression (data not shown) were slightly but not significantly decreased in 48-wk-old IRS-2$^{-/-}$Tg2576 animals (Fig. 2*C*).

IGF-1R deficiency rescues APP^{SW}-induced mortality

Given that evolutionary diversification has resulted in the emergence of the mammalian IR and IGF-1R as orthologs of DAF-2 and that IRS-2 acts as a signaling

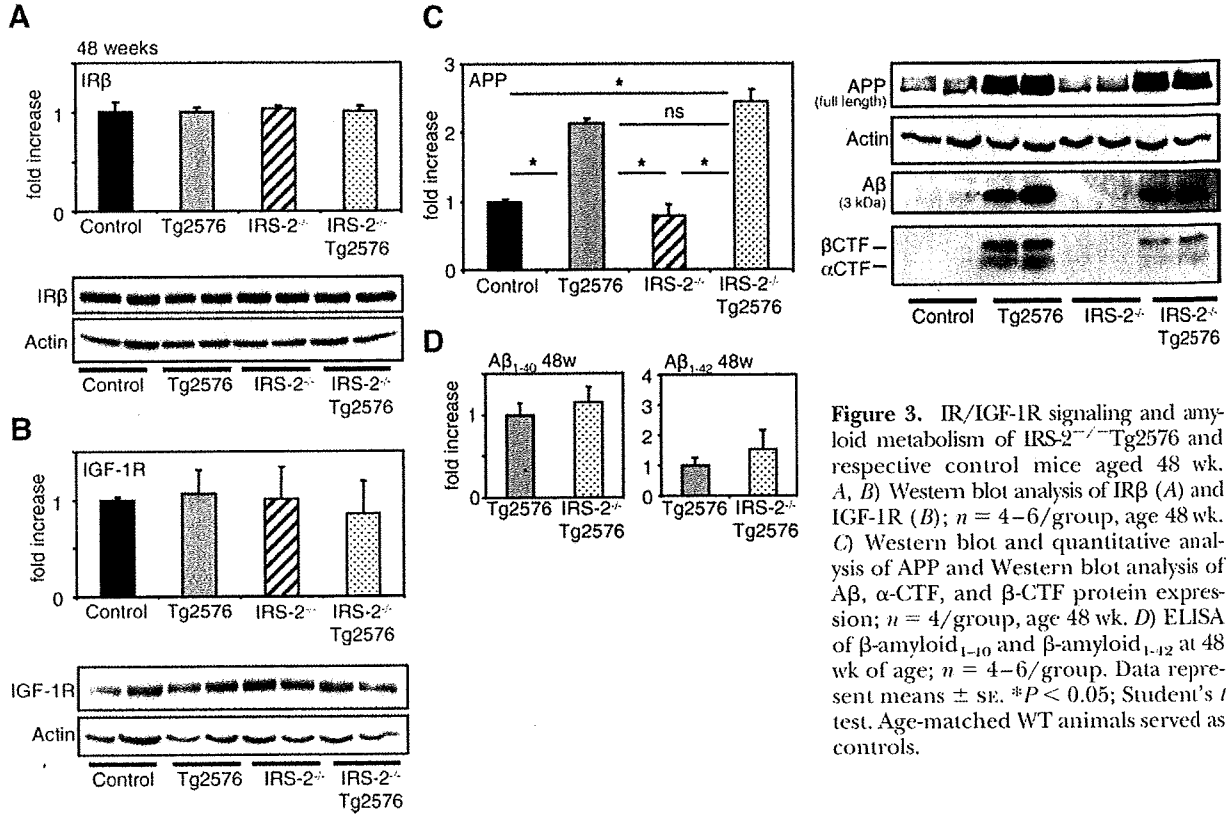

Figure 3. IR/IGF-1R signaling and amyloid metabolism of IRS-2$^{-/-}$Tg2576 and respective control mice aged 48 wk. *A*, *B*) Western blot analysis of IRβ (*A*) and IGF-1R (*B*); $n = 4-6$/group, age 48 wk. *C*) Western blot and quantitative analysis of APP and Western blot analysis of Aβ, α-CTF, and β-CTF protein expression; $n = 4$/group, age 48 wk. *D*) ELISA of β-amyloid$_{1-40}$ and β-amyloid$_{1-42}$ at 48 wk of age; $n = 4-6$/group. Data represent means ± SE. $^*P < 0.05$; Student's *t* test. Age-matched WT animals served as controls.

mediator not only in the IR/IGF-1R pathway, we next aimed to identify the upstream signal responsible for IRS-2-mediated control of AD-associated mortality. Moreover, since IRS-2 deficiency in the former model occurred body-wide and apparently was organismal, and IRS-2 deficiency resulting in hyperglycemia potentially counteracted the effect of IRS-2-deficiency on Aβ processing and deposition, we directly addressed the role of neuronal IR/IGF-1 resistance on AD-associated mortality.

To this end, we generated neuron-specific IGF-1R-knockout mice. To achieve neuron-specific deletion, we crossed mice carrying the floxed exon 3 of the IGF-1R gene with mice expressing the Cre-recombinase under control of the synapsin-1 promoter (Syn-Cre). Using a Rosa-26 reporter line, Cre expression was predominantly found in the dentate gyrus, CA3 region of the hippocampus, and amygdala, and very low expression in the piriform cortex, neocortex, and thalamus (**Fig. 4***A*). However, Western blot analysis revealed a significant reduction of IGF-1R expression only in isolated hippocampi, whereas different cortical regions, cerebellum, and total brain did not show significant IGF-1R alteration (data not shown). On the other hand, IR expression in the hippocampus and cortex was unaltered (Fig. 4*C*). Furthermore, IGF-1R and IR protein expression in muscle, kidney, heart, lung, fat, pancreas, and lung was indistinguishable between WT and nIGF-1R$^{-/-}$ mice (data not shown). Consistent with IGF-1 resistance in nIGF-1R$^{-/-}$ mice, AKT phosphorylation at Ser-473 was reduced following stimulation of isolated hippocampi with IGF-1 (Fig. 4*C*). However, basal AKT phosphorylation was unchanged in nIGF-1$^{-/-}$ hippocampi compared to WT hippocampi.

To further analyze the influence of IGF-1R deletion predominantly in the hippocampus on APP^{SW}-induced lethality, we crossed nIGF-R$^{-/-}$ mice in a Tg2576 background and performed Kaplan-Meier analyses of the different genotypes up to the age of 60 wk. These analyses revealed that both female and male nIGF-1R$^{-/-}$ mice are largely protected against APP^{SW}-induced lethality (Fig. 4*B*). As expected, IGF-1R deficiency predominantly in the hippocampus did not affect somatic growth or glucose metabolism in either gender (Fig. 4*D*, *E*). Also, insulin- and glucose-tolerance tests remained unchanged (Fig. 4*F*, *G*), further supporting the notion that systemic hyperglycemia counteracts the positive role of neuronal IGF-1-resistance in male IRS-2$^{-/-}$Tg2576 mice.

In hippocampi of nIGF-1R$^{-/-}$Tg2576 mice aged 28 wk, α- and β-CTF were significantly reduced compared to Tg2576 mice (**Fig. 5***A*). In contrast, analysis of cortices of these mice showed unchanged expression of α-/β-CTF (Fig. 5*A*, *B*). Consistent with a direct role of neuron-autonomous IGF-1/IRS-2-mediated control of APP metabolism, nIGF-1R$^{-/-}$Tg2576 mice showed reduced Aβ$_{1-40}$ occurrence specifically in the hippocampus, but not in other brain regions (Fig. 5*C*). Analysis of downstream IR/IGF-1R signaling proteins (*e.g.*, Akt, GSK-3β, and ERK-1/2) revealed an unchanged expression. Furthermore, there was no difference in basal phosphorylation of these proteins (pAKT^{Ser473}, pGSK-3β^{Ser9}, and pERK-1/2$^{Thr202/Tyr204}$) in nIGF-1R$^{-/-}$Tg2576 mice compared to Tg2576, and IDE

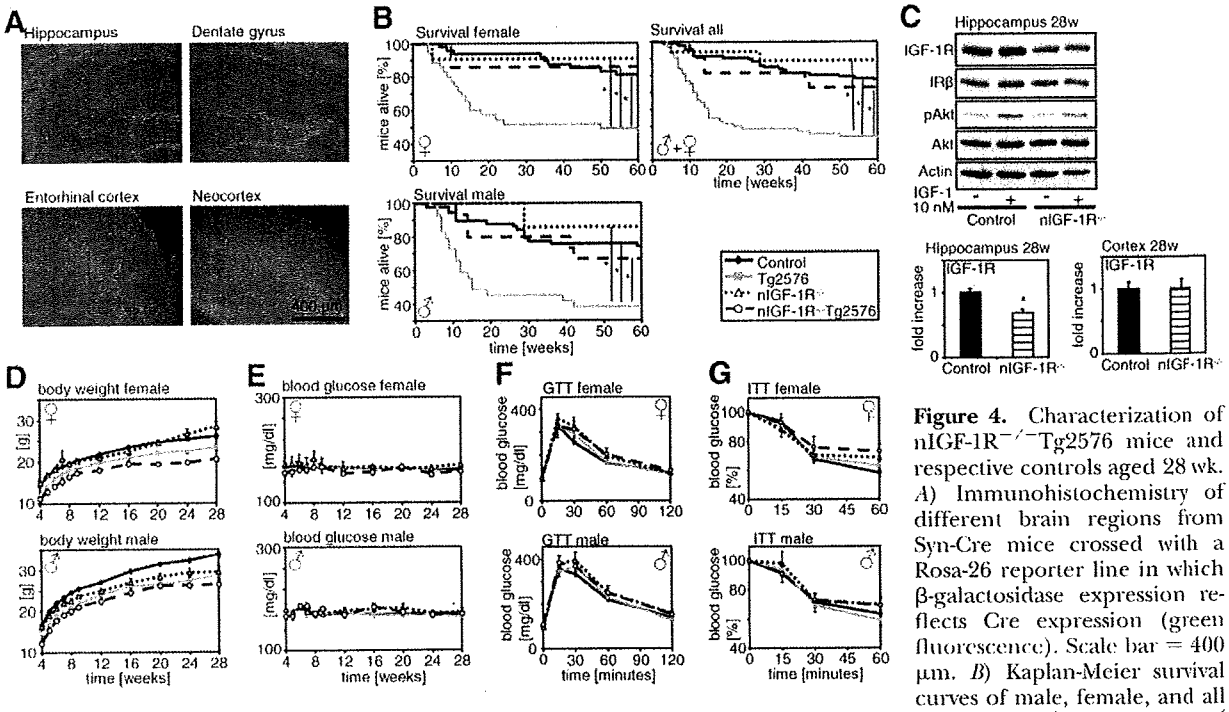

Figure 4. Characterization of nIGF-1R$^{-/-}$Tg2576 mice and respective controls aged 28 wk. *A*) Immunohistochemistry of different brain regions from Syn-Cre mice crossed with a Rosa-26 reporter line in which β-galactosidase expression reflects Cre expression (green fluorescence). Scale bar = 400 μm. *B*) Kaplan-Meier survival curves of male, female, and all nIGF-1R$^{-/-}$Tg2576 mice. Survival was assessed from 109 female (53 control, 37 Tg2576, 9 nIGF-1R$^{-/-}$, 11 nIGF-1R$^{-/-}$Tg2576) and 100 male mice (59 control, 24 Tg2576, 9 nIGF-1$^{-/-}$, 18 nIGF-1R$^{-/-}$Tg2576). $^{*}P < 0.05$; Wilcoxon rank test. *C*) *Ex vivo* IGF-1-stimulation of hippocampi from nIGF-1R$^{-/-}$ mice and respective controls with 10 nM IGF-1 and following Western blot analysis of IR signaling cascade. IGF-1 receptor protein expression from isolated hippocampi was quantified using densitometry; $n = 5$/group. *D–G*) Body weight measurement (*D*), blood glucose measurement (*E*), insulin-tolerance tests (ITT) (*F*), and glucose-tolerance tests (GTT) (*G*). ITT and GTT were performed in 115 female (58 control, 34 Tg2576, 15 nIGF-1$^{-/-}$, 8 nIGF-1R$^{-/-}$Tg2576) and 110 male mice (62 control, 23 Tg2576, 10 nIGF-1R$^{-/-}$, 15 nIGF-1R$^{-/-}$Tg2576). Data represent means ± SE. Age-matched animals without APP^{SW} and/or Syn-Cre expression served as controls.

expression remained unchanged in brain lysates of nIGF-1R$^{-/-}$Tg2576 mice (Fig. 5*D*).

Analysis of α- and β-CTF as well as $A\beta_{1-40}$ and $A\beta_{1-42}$ in hippocampi and cortices from nIGF-1R$^{-/-}$Tg2576 mice aged 60 wk (**Fig. 6*A*, *B***) revealed a reduction of α- and β-CTF specifically in the hippocampus as observed in 28-wk-old mice (Fig. 5*B*). In contrast to IRS-2$^{-/-}$Tg2576 mice, hippocampi of IGF-1R$^{-/-}$Tg2576 mice showed a reduction of $A\beta_{1-40}$ and $A\beta_{1-42}$ even in 60-wk-old mice, suggesting that complete IGF-1 resistance exerts long-term effects on Aβ accumulation (Fig. 6*B*).

Heterozygous IGF-1R deficiency and IR deficiency do not affect survival of Tg2576 mice

To further elucidate whether the neuronal IR deficiency or heterozygosity for the IGF-1R might influence survival of Tg2576 mice, we performed Kaplan-Meier analysis on heterozygous IGF-1R-deficient mice (nIGF-1R$^{+/-}$) and neuron-specific IR-deficient mice (nIR$^{-/-}$) in a Tg2576 background. However, heterozygosity for IGF-1R partially rescues the APP^{SW}-induced mortality in either gender, but the tendency to increased survival of nIGF-1R$^{+/-}$Tg2576 mice failed to reach statistical significance, even though 24 nIGF-1R$^{+/-}$Tg2576 and 71 Tg2576 mice have been followed up (**Fig. 7*A***). Moreover, neuronal specific knockout of the IR using the same Cre (synapsin-1 Cre) showed no influence on Tg2576 mortality in male and female mice (Fig. 7*B*). In both mouse models, growth and glucose metabolism were not affected (data not shown).

Thus, only a homozygous deletion of the IGF-1R in the described brain regions is capable of rescuing premature mortality in Tg2576 mice.

DISCUSSION

The present study reveals several novel insights into the highly debated interaction of neuronal insulin/IGF-1 resistance and the pathophysiology of neurodegenerative disorders. Primarily, clinical association studies have nurtured the hypothesis that insulin resistance, aside from afflicting peripheral organs and causing metabolic disturbances found in diabetes, affects the CNS, leading to the formation of neurodegenerative diseases that are more frequently associated with T2DM. Here we demonstrate that, unexpectedly, IGF-1 resistance in the CNS in the absence of metabolic disturbances prevents mortality as the most dramatic end point of experimental AD in Tg2576 mice (female/euglycemic male IRS-2$^{-/-}$Tg2576 and female/male nIGF-1R$^{-/-}$Tg2576 mice). In contrast, overt hyperglycemia as present in male IRS-2$^{-/-}$Tg2576 mice is

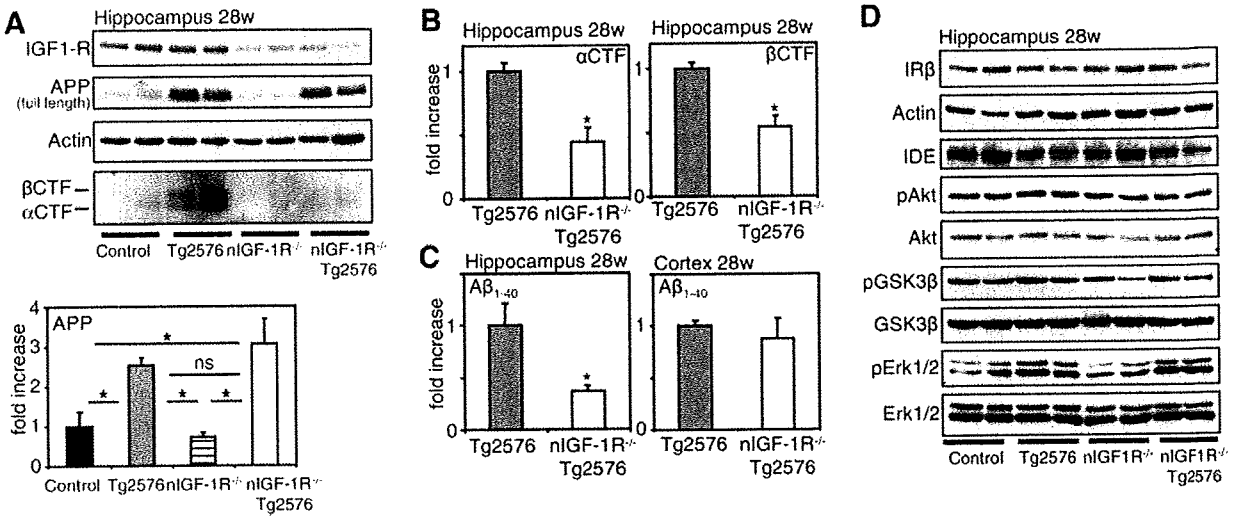

Figure 5. IR/IGF-1R signaling and amyloid metabolism of nIGF-1R$^{-/-}$Tg2576 and respective control mice aged 28 wk. *A*) Western blot and quantitative analysis of hippocampal expression of APP; Western blot analysis of IGF-1 receptor, α-CTF, and β-CTF; $n = 4$/group, age 28 wk. *B*) Quantitative analysis of α-CTF and β-CTF; $n = 4$/group, age 28 wk. *C*) ELISA of β-amyloid$_{1-40}$ in hippocampus and cortex; $n = 4$/group, age 28 wk. *D*) Western blot analysis of IRβ, IDE, pAkt, pGSK-3β, pErk-1/2, and respective loading controls, age 28 wk. Data represent means ± SE. Age-matched animals without APP^{SW} and/or Syn-Cre expression served as controls. $^*P < 0.05$; Student's *t* test.

sufficient to overcome the protective effect of neuronal insulin/IGF-1 resistance. These experiments clearly indicate that either hyperglycemia *per se* or vascular complications resulting from uncontrolled hyperglycemia explain the association of T2DM with AD, rather than a common underlying phenomenon of insulin resistance. This notion is in line with the observation that an increased AD risk correlates with impaired insulin secretion (37) and increased levels of glycosylated HbA1c as a marker for hyperglycemia (38, 39).

However, there are certain limitations of the present study. In IRS-2$^{-/-}$ and Tg2576 mice, the genetic background influences phenotypes. Male IRS-2$^{-/-}$ mice on a pure C57BL/6 background develop early severe diabetes mellitus, and most die within 6 mo of age, whereas male IRS-2$^{-/-}$ mice on mixed genetic background present with a milder metabolic phenotype and survive (20, 31). Furthermore, up to 80% of pure C57BL/6 mice develop spontaneous hyperglycemia in the first 6 mo, possibly influencing longevity (31, 40). Previous studies on APP-overexpressing mice have shown that lethality is influenced by the genetic background (21). Since nearly all Tg2576 mice on a pure C57BL/6 background die within the first months, it is impossible to investigate amyloid accumulation or IR/IGF-1R signaling in a pure C57BL/6 background (21). The hybrid background used in the present study enabled us to investigate APP^{SW}-induced lethality, amyloid accumulation, and IR/IGF-1R signaling in different brain regions in the same mouse strain without the influence of spontanous hyperglyemia in the control groups. However, it must be mentioned that the results presented here might not completely be conferrable to other genetic backgrounds. Furthermore, in our intercrosses there was an unusual high mortality in male controls during the first months. We speculate that an

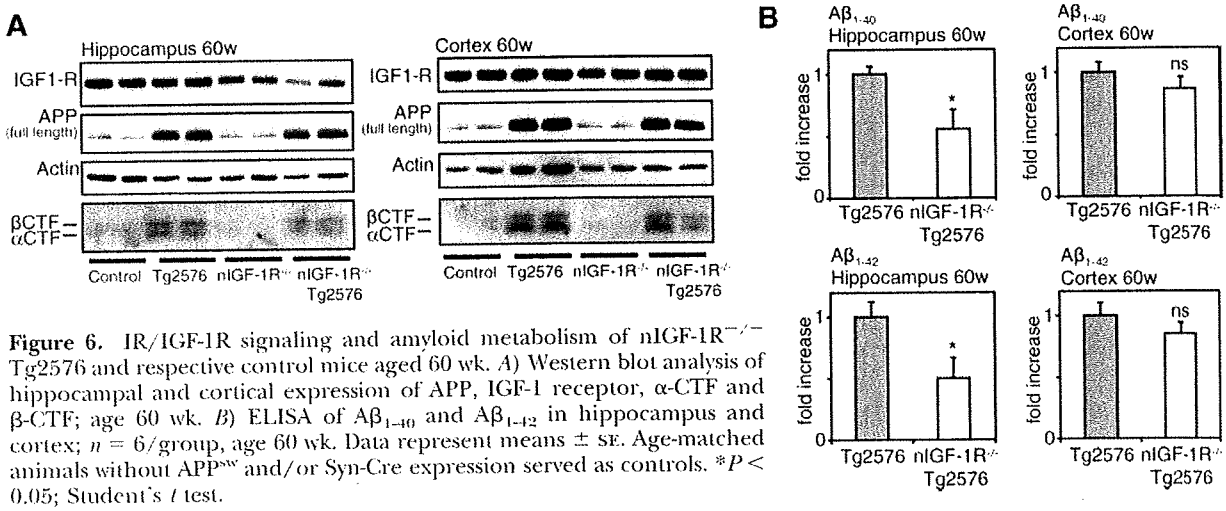

Figure 6. IR/IGF-1R signaling and amyloid metabolism of nIGF-1R$^{-/-}$ Tg2576 and respective control mice aged 60 wk. *A*) Western blot analysis of hippocampal and cortical expression of APP, IGF-1 receptor, α-CTF and β-CTF; age 60 wk. *B*) ELISA of Aβ$_{1-40}$ and Aβ$_{1-42}$ in hippocampus and cortex; $n = 6$/group, age 60 wk. Data represent means ± SE. Age-matched animals without APP^{SW} and/or Syn-Cre expression served as controls. $^*P < 0.05$; Student's *t* test.

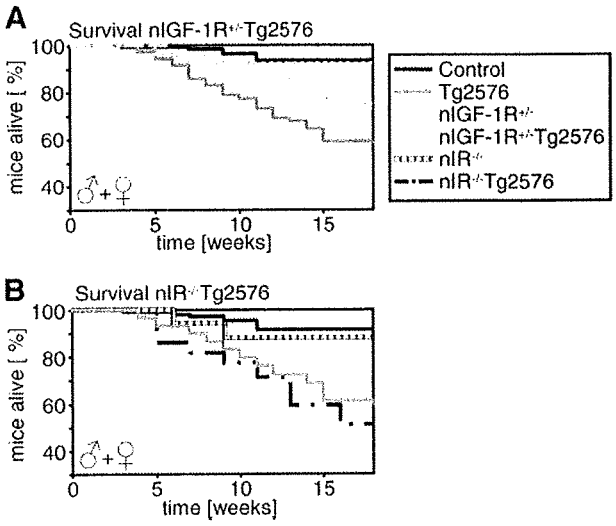

Figure 7. Kaplan-Meier analysis of nIGF-1R$^{+/-}$Tg2576 and nIR$^{-/-}$Tg2576 mice aged 18 wk with respective controls up to the age of 18 wk. *A*) Kaplan-Meier analysis. Survival was assessed from 278 female and male mice (137 WT, 71 Tg2576, 26 IGF-1R$^{+/-}$, 24 IGF-1R$^{+/-}$Tg2576). *B*) Kaplan-Meier analysis. Survival was assessed from 188 female and male mice (90 WT, 59 Tg2576, 17 IR$^{-/-}$, 22 IR$^{-/-}$Tg2576).

unknown environmental factor might be responsible for this relatively high mortality.

IR and IGF-1R signaling is markedly disturbed in the CNS of patients with AD (11–13). The overall expression of IGF-1R is reduced in AD brains, dependent on the severity of the disease. Moreover, brain IGF-1 mRNA levels are diminished in late AD, whereas IGF-1 serum levels are increased in early stages of disease, suggesting that IGF-1 resistance plays a role in the pathogenesis of AD (14, 41). IRS-1/2 protein expression decreases with severity of neurodegeneration in AD brains, and the inhibiting phosphorylation of IRS-1 at Ser-312 and Ser-616 is increased, leading to impaired IR and IGF-1R signaling (13). Thus, IR/IGF-1R downstream signal transduction is impaired in AD brains, leading to the hypothesis that cerebral insulin/IGF-1 resistance might be involved in the pathogenesis of AD. However, it is still unclear whether these changes are cause or consequence of disease.

In fact, the current observation that neuron and even hippocampus restricted IGF-1 resistance (but not insulin resistance) protects from AD-associated mortality argues for an evolutionary conserved life-extending mechanism from *C. elegans* to mice. In *C. elegans*, neuronal DAF-2 controls longevity (42). Furthermore, haploinsufficiency for the IGF-1R (43, 44) as well as CNS-restricted IRS-2 deficiency (30) extends life span in mice. Moreover, impairing insulin/IGF-1-like signaling in *C. elegans* reduces Aβ-proteotoxicity by FOXO-dependent as well as FOXO-independent mechanisms (20). While the lifespan-extending effect of IGF-1 resistance and neuronal IRS-2 deficiency seems to improve defense against reactive oxygen species, inhibition of AD-associated mortality in the present models appears to be linked to IGF-1R-mediated processing of Aβ.

Aβ consists of small peptides with N- and C-terminal heterogeneity, that is, $A\beta_{1-40}$ and $A\beta_{1-42}$, which are proteolytically released from APP *via* sequential cleavage by the β- and γ-secretases (45–47). Initial β-secretase cleavage generates a soluble fragment from the NH_2 terminus of APP, while the β-CTF stays membrane bound. α-Secretase cleavage leads to membrane-bound α-CTF (48). Interestingly, in IRS-2$^{-/-}$Tg2576 and nIGF-1R$^{-/-}$Tg2576 mice, β-CTFs occur at significantly lower levels, which suggests decreased β-cleavage in these models. Accordingly, amyloid accumulation is delayed in IRS-2$^{-/-}$Tg2576 mice compared to WT. In SHSY5Y cells as well as in primary cultured neurons, chronic treatment with IGF-1 causes a switch from TrkA to $p75^{NTR}$ expression as seen in aging brains (35). This switch might increase β-secretase activity indirectly by activation of neuronal sphingomyelinase, which is responsible for active liberation of the second messenger ceramide (49), stabilizing BACE-1 at least in SHSY5Y cells (50). This process has been proposed to be responsible for the effect of IGF-1 on Aβ generation. However, BACE-1 expression and BACE-1 activity are not altered in our models, which suggests that either marginal reduction of BACE-1 activity or an unknown mechanism regulated by IGF-1R/IRS-2-mediated signals is responsible for the decreased APP processing observed in IRS-2$^{-/-}$Tg2576 and nIGF-1R$^{-/-}$Tg2576 mice. Further research is needed to elucidate the role of IGF-1R signaling in the regulation of APP cleavage.

At least 4 independent reports linked β-amyloid accumulation to survival of APP-overexpressing mice (22–24, 32, 51). Transgenic expression of IDE or neprilysin in neurons reduces brain Aβ levels and prevents amyloid plaque formation and premature death in APP transgenic animals (32). On the other hand, chemokine receptor Ccr2 deficiency accelerates early disease progression by markedly impaired microglial activation. In Tg2576 mice deficient for Ccr2, accumulation of Aβ occurred earlier, and these mice died significantly sooner compared to Tg2576 (23). These data suggest that the amount of Aβ might be partially responsible for the decreased mortality in our IGF-1-resistant models. Concerning insulin/IGF-1 resistance, it has been shown that IDE expression as an "amyloid-degrading" enzyme is stimulated by IR/IGF-1R cascade (52). However, we could not detect any changes in IDE expression in our models.

According to numerous studies, IRs and IGF-1Rs as well as IRS-1 and IRS-2 are widely distributed throughout the developing and mature brain (53–58). The highest IR density is found in the olfactory bulb, hippocampal formation, hypothalamus, and cerebral cortex. IGF-1R is highly expressed in the hippocampus, amygdala, parahippocampal gyrus, and cortex (59). The two receptors particularly overlap in their expression in the dentate gyrus of the hippocampal formation and amygdala and in distinct areas of the cortex. Even though the intracellular signaling network of these two receptors is nearly undistinguishable, the physiological role of both receptors is obviously different. In our model, conditional IGF-1R- but not IR-knockout using the same Cre line (synapsin-1 Cre) rescues premature lethality of Tg2576 mice. However, the molecular mechanisms need to be elucidated.

Thus, the currently propagated approach to improve symptoms of AD by intranasal application of insulin (60) may prove detrimental for the survival of patients with AD. Further analysis of the downstream mediators of hippocampus IGF-1R/IRS-2-mediated signaling in control of AD-associated mortality may therefore set the ground for novel therapeutic interventions against AD.

Taken together, we demonstrate that neuronal IGF-1R/IRS-2 deficiency protects against APP^{SW}-induced lethality, neuronal IRS-2 deficiency delays Aβ accumulation *in vivo*, and homozygous neuronal deletion of IGF-1R-mediated signals reduces Aβ accumulation even in aged mice.

Thus, down-regulation of IGF-1R and IRS-2 observed in neurons of patients with AD is most likely a compensatory phenomenon to decrease amyloid burden and prolongate survival. A similar mechanism with down-regulation of serum IGF-1 levels has been previously suggested in response to chronic DNA damage (61). FJ

This work was supported by the Fritz-Thyssen Foundation (AZ 10.06.2.209) and Alzheimer Forschungs-Initiative e.V. (08813) to M.S. and by funds to J.C.B. by the Deutsche Forschungsgemeinschaft (Br-1492–7) and the Fritz-Thyssen Foundation. We gratefully thank Prof. R. Wiesner and Prof. C. Niessen for helpful discussions on the data and the manuscript.

REFERENCES

1. Cole, A. R., Astell, A., Green, C., and Sutherland, C. (2007) Molecular connexions between dementia and diabetes. *Neurosci. Biobehav. Rev.* **31,** 1046–1063
2. Tschanz, J. T., Corcoran, C., Skoog, I., Khachaturian, A. S., Herrick, J., Hayden, K. M., Welsh-Bohmer, K. A., Calvert, T., Norton, M. C., Zandi, P., and Breitner, J. C. (2004) Dementia: the leading predictor of death in a defined elderly population: the Cache County Study. *Neurology* **62,** 1156–1162
3. Ott, A., Stolk, R. P., van Harskamp, F., Pols, H. A., Hofman, A., and Breteler, M. M. (1999) Diabetes mellitus and the risk of dementia: the Rotterdam Study. *Neurology* **53,** 1937–1942
4. Luchsinger, J. A., Tang, M. X., Shea, S., and Mayeux, R. (2004) Hyperinsulinemia and risk of Alzheimer disease. *Neurology* **63,** 1187–1192
5. Haan, M. N. (2006) Therapy insight: type 2 diabetes mellitus and the risk of late-onset Alzheimer's disease. *Nat. Clin. Pract. Neurol.* **2,** 159–166
6. Stewart, R., and Liolitsa, D. (1999) Type 2 diabetes mellitus, cognitive impairment and dementia. *Diabetes Med.* **16,** 93–112
7. Lovestone, S. (1999) Diabetes and dementia: is the brain another site of end-organ damage? *Neurology* **53,** 1907–1909
8. Steen, E., Terry, B. M., Rivera, E. J., Cannon, J. L., Neely, T. R., Tavares, R., Xu, X. J., Wands, J. R., and de la Monte, S. M. (2005) Impaired insulin and insulin-like growth factor expression and signaling mechanisms in Alzheimer's disease: is this type 3 diabetes? *J. Alzheimers Dis.* **7,** 63–80
9. De la Monte, S. M., Tong, M., Lester-Coll, N., Plater, M., Jr., and Wands, J. R. (2006) Therapeutic rescue of neurodegeneration in experimental type 3 diabetes: relevance to Alzheimer's disease. *J. Alzheimers Dis.* **10,** 89–109
10. Pilcher, H. (2006) Alzheimer's disease could be "type 3 diabetes." *Lancet Neurol.* **5,** 388–389
11. Frolich, L., Blum-Degen, D., Bernstein, H. G., Engelsberger, S., Humrich, J., Laufer, S., Muschner, D., Thalheimer, A., Turk, A., Hoyer, S., Zochling, R., Boissl, K. W., Jellinger, K., and Riederer, P. (1998) Brain insulin and insulin receptors in aging and sporadic Alzheimer's disease. *J. Neural Transm.* **105,** 423–438
12. Frolich, L., Blum-Degen, D., Riederer, P., and Hoyer, S. (1999) A disturbance in the neuronal insulin receptor signal transduction in sporadic Alzheimer's disease. *Ann. N. Y. Acad. Sci.* **893,** 290–293
13. Moloney, A. M., Griffin, R. J., Timmons, S., O'Connor, R., Ravid, R., and O'Neill, C. (2008) Defects in IGF-1 receptor, insulin receptor and IRS-1/2 in Alzheimer's disease indicate possible resistance to IGF-1 and insulin signalling. [E-pub ahead of print] *Neurobiol. Aging* doi: 10.1016/j.neurobiolaging.2008.04.002
14. Rivera, E. J., Goldin, A., Fulmer, N., Tavares, R., Wands, J. R., and de la Monte, S. M. (2005) Insulin and insulin-like growth factor expression and function deteriorate with progression of Alzheimer's disease: link to brain reductions in acetylcholine. *J. Alzheimers Dis.* **8,** 247–268
15. Finch, C. E., and Ruvkun, G. (2001) The genetics of aging. *Annu. Rev. Genomics Hum. Genet.* **2,** 435–462
16. Kenyon, C., Chang, J., Gensch, E., Rudner, A., and Tabtiang, R. (1993) A C. elegans mutant that lives twice as long as wild type. *Nature* **366,** 461–464
17. Kimura, K. D., Tissenbaum, H. A., Liu, Y., and Ruvkun, G. (1997) daf-2, an insulin receptor-like gene that regulates longevity and diapause in *Caenorhabditis elegans*. *Science* **277,** 942–946
18. Wadsworth, W. G., and Riddle, D. L. (1989) Developmental regulation of energy metabolism in *Caenorhabditis elegans*. *Dev. Biol.* **132,** 167–173
19. Cohen, E., Bieschke, J., Perciavalle, R. M., Kelly, J. W., and Dillin, A. (2006) Opposing activities protect against age-onset proteotoxicity. *Science* **313,** 1604–1610
20. Kubota, N., Tobe, K., Terauchi, Y., Eto, K., Yamauchi, T., Suzuki, R., Tsubamoto, Y., Komeda, K., Nakano, R., Miki, H., Satoh, S., Sekihara, H., Sciacchitano, S., Lesniak, M., Aizawa, S., Nagai, R., Kimura, S., Akanuma, Y., Taylor, S. I., and Kadowaki, T. (2000) Disruption of insulin receptor substrate 2 causes type 2 diabetes because of liver insulin resistance and lack of compensatory beta-cell hyperplasia. *Diabetes* **49,** 1880–1889
21. Carlson, G. A., Borchelt, D. R., Dake, A., Turner, S., Danielson, V., Coffin, J. D., Eckman, C., Meiners, J., Nilsen, S. P., Younkin, S. G., and Hsiao, K. K. (1997) Genetic modification of the phenotypes produced by amyloid precursor protein overexpression in transgenic mice. *Hum. Mol. Genet.* **6,** 1951–1959
22. Matsubara, E., Bryant-Thomas, T., Pacheco, Q. J., Henry, T. L., Poeggeler, B., Herbert, D., Cruz-Sanchez, F., Chyan, Y. J., Smith, M. A., Perry, G., Shoji, M., Abe, K., Leone, A., Grundke-Ikbal, I., Wilson, G. L., Ghiso, J., Williams, C., Refolo, L. M., Pappolla, M. A., Chain, D. G., and Neria, E. (2003) Melatonin increases survival and inhibits oxidative and amyloid pathology in a transgenic model of Alzheimer's disease. *J. Neurochem.* **85,** 1101–1108
23. El Khoury, J., Toft, M., Hickman, S. E., Means, T. K., Terada, K., Geula, C., and Luster, A. D. (2007) Ccr2 deficiency impairs microglial accumulation and accelerates progression of Alzheimer-like disease. *Nat. Med.* **13,** 432–438
24. Nathan, C., Calingasan, N., Nezezon, J., Ding, A., Lucia, M. S., La Perle, K., Fuortes, M., Lin, M., Ehrt, S., Kwon, N. S., Chen, J., Vodovotz, Y., Kipiani, K., and Beal, M. F. (2005) Protection from Alzheimer's-like disease in the mouse by genetic ablation of inducible nitric oxide synthase. *J. Exp. Med.* **202,** 1163–1169
25. Bruning, J. C., Gautam, D., Burks, D. J., Gillette, J., Schubert, M., Orban, P. C., Klein, R., Krone, W., Muller-Wieland, D., and Kahn, C. R. (2000) Role of brain insulin receptor in control of body weight and reproduction. *Science* **289,** 2122–2125
26. Stachelscheid, H., Ibrahim, H., Koch, L., Schmitz, A., Tscharntke, M., Wunderlich, F. T., Scott, J., Michels, C., Wickenhauser, C., Haase, I., Bruning, J. C., and Niessen, C. M. (2008) Epidermal insulin/IGF-1 signalling control interfollicular morphogenesis and proliferative potential through Rac activation. *EMBO J.* **27,** 2091–2101
27. Seibler, J., Zevnik, B., Kuter-Luks, B., Andreas, S., Kern, H., Hennek, T., Rode, A., Heimann, C., Faust, N., Kauselmann, G., Schoor, M., Jaenisch, R., Rajewsky, K., Kuhn, R., and Schwenk, F. (2003) Rapid generation of inducible mouse mutants. *Nucleic Acids Res.* **31,** e12
28. Hsiao, K., Chapman, P., Nilsen, S., Eckman, C., Harigaya, Y., Younkin, S., Yang, F., and Cole, G. (1996) Correlative memory deficits, Abeta elevation, and amyloid plaques in transgenic mice. *Science* **274,** 99–102
29. Stein, T. D., and Johnson, J. A. (2002) Lack of neurodegeneration in transgenic mice overexpressing mutant amyloid precur-

sor protein is associated with increased levels of transthyretin and the activation of cell survival pathways. *J. Neurosci.* **22,** 7380–7388
30. Taguchi, A., Wartschow, L. M., and White, M. F. (2007) Brain IRS2 signaling coordinates life span and nutrient homeostasis. *Science* **317,** 369–372
31. Selman, C., Lingard, S., Choudhury, A. I., Batterham, R. L., Claret, M., Clements, M., Ramadani, F., Okkenhaug, K., Schuster, E., Blanc, E., Piper, M. D., Al Qassab, H., Speakman, J. R., Carmignac, D., Robinson, I. C., Thornton, J. M., Gems, D., Partridge, L., and Withers, D. J. (2008) Evidence for lifespan extension and delayed age-related biomarkers in insulin receptor substrate 1 null mice. *FASEB J.* **22,** 807–818
32. Leissring, M. A., Farris, W., Chang, A. Y., Walsh, D. M., Wu, X., Sun, X., Frosch, M. P., and Selkoe, D. J. (2003) Enhanced proteolysis of beta-amyloid in APP transgenic mice prevents plaque formation, secondary pathology, and premature death. *Neuron* **40,** 1087–1093
33. Burks, D. J., de Mora, J. F., Schubert, M., Withers, D. J., Myers, M. G., Towery, H. H., Altamuro, S. L., Flint, C. L., and White, M. F. (2000) IRS-2 pathways integrate female reproduction and energy homeostasis. *Nature* **407,** 377–382
34. Adlerz, L., Holback, S., Multhaup, G., and Iverfeldt, K. (2007) IGF-1-induced processing of the amyloid precursor protein family is mediated by different signaling pathways. *J. Biol. Chem.* **282,** 10203–10209
35. Costantini, C., Scrable, H., and Puglielli, L. (2006) An aging pathway controls the TrkA to p75NTR receptor switch and amyloid beta-peptide generation. *EMBO J.* **25,** 1997–2006
36. McConlogue, L., Buttini, M., Anderson, J. P., Brigham, E. F., Chen, K. S., Freedman, S. B., Games, D., Johnson-Wood, K., Lee, M., Zeller, M., Liu, W., Motter, R., and Sinha, S. (2007) Partial reduction of BACE1 has dramatic effects on Alzheimer plaque and synaptic pathology in APP transgenic mice. *J. Biol. Chem.* **282,** 26326–26334
37. Ronnemaa, E., Zethelius, B., Sundelof, J., Sundstrom, J., Degerman-Gunnarsson, M., Berne, C., Lannfelt, L., and Kilander, L. (2008) Impaired insulin secretion increases the risk of Alzheimer disease. *Neurology* **71,** 1065–1071
38. Whitmer, R. A., Selby, J. V., Van Den Eeden, S. K., Haan, M. N., Quesenberry, Jr., C. P., Minkoff, J., and Yaffe, K. (2006) Glycemic control and risk of dementia in a cohort of patients with type 2 diabetes. *Alzheimers Dement.* **2,** S149
39. Cukierman-Yaffe, T., Gerstein, H. C., Williamson, J. D., Lazar, R. M., Lovato, L., Miller, M. E., Coker, L. H., Murray, A., Sullivan, M. D., Marcovina, S. M., and Launer, L. J. (2009) Relationship between baseline glycemic control and cognitive function in individuals with type 2 diabetes and other cardiovascular risk factors: the action to control cardiovascular risk in diabetes-memory in diabetes (ACCORD-MIND) trial. *Diabetes Care* **32,** 221–226
40. Doria, A., Patti, M. E., and Kahn, C. R. (2008) The emerging genetic architecture of type 2 diabetes. *Cell. Metab.* **8,** 186–200
41. Vardy, E. R., Rice, P. J., Bowie, P. C., Holmes, J. D., Grant, P. J., and Hooper, N. M. (2007) Increased circulating insulin-like growth factor-1 in late-onset Alzheimer's disease. *J. Alzheimers Dis.* **12,** 285–290
42. Wolkow, C. A., Kimura, K. D., Lee, M. S., and Ruvkun, G. (2000) Regulation of C. elegans life-span by insulin-like signaling in the nervous system. *Science* **290,** 147–150
43. Holzenberger, M., Dupont, J., Ducos, B., Leneuve, P., Geloen, A., Even, P. C., Cervera, P., and Le Bouc, Y. (2003) IGF-1 receptor regulates lifespan and resistance to oxidative stress in mice. *Nature* **421,** 182–187
44. Kappeler, L., Filho, C. M., Dupont, J., Leneuve, P., Cervera, P., Perin, L., Loudes, C., Blaise, A., Klein, R., Epelbaum, J., Le Bouc, Y., and Holzenberger, M. (2008) Brain IGF-1 receptors control mammalian growth and lifespan through a neuroendocrine mechanism. *PLoS Biol.* **6,** e254
45. Kang, J., Lemaire, H. G., Unterbeck, A., Salbaum, J. M., Masters, C. L., Grzeschik, K. H., Multhaup, G., Beyreuther, K., and Muller-Hill, B. (1987) The precursor of Alzheimer's disease amyloid A4 protein resembles a cell-surface receptor. *Nature* **325,** 733–736
46. Vassar, R., Bennett, B. D., Babu-Khan, S., Kahn, S., Mendiaz, E. A., Denis, P., Teplow, D. B., Ross, S., Amarante, P., Loeloff, R., Luo, Y., Fisher, S., Fuller, J., Edenson, S., Lile, J., Jarosinski, M. A., Biere, A. L., Curran, E., Burgess, T., Louis, J. C., Collins, F., Treanor, J., Rogers, G., and Citron, M. (1999) Beta-secretase cleavage of Alzheimer's amyloid precursor protein by the transmembrane aspartic protease BACE. *Science* **286,** 735–741
47. Lorenzo, A., and Yankner, B. A. (1994) Beta-amyloid neurotoxicity requires fibril formation and is inhibited by Congo red. *Proc. Natl. Acad. Sci. U. S. A.* **91,** 12243–12247
48. Lammich, S., Kojro, E., Postina, R., Gilbert, S., Pfeiffer, R., Jasionowski, M., Haass, C., and Fahrenholz, F. (1999) Constitutive and regulated alpha-secretase cleavage of Alzheimer's amyloid precursor protein by a disintegrin metalloprotease. *Proc. Natl. Acad. Sci. U. S. A.* **96,** 3922–3927
49. Puglielli, L. (2008) Aging of the brain, neurotrophin signaling, and Alzheimer's disease: is IGF1-R the common culprit? *Neurobiol. Aging* **29,** 795–811
50. Puglielli, L., Ellis, B. C., Saunders, A. J., and Kovacs, D. M. (2003) Ceramide stabilizes beta-site amyloid precursor protein-cleaving enzyme 1 and promotes amyloid beta-peptide biogenesis. *J. Biol. Chem.* **278,** 19777–19783
51. Meilandt, W. J., Cisse, M., Ho, K., Wu, T., Esposito, L. A., Scearce-Levie, K., Cheng, I. H., Yu, G. Q., and Mucke, L. (2009) Neprilysin overexpression inhibits plaque formation but fails to reduce pathogenic Aβ oligomers and associated cognitive deficits in human amyloid precursor protein transgenic mice. *J. Neurosci.* **29,** 1977–1986
52. Zhao, L., Teter, B., Morihara, T., Lim, G. P., Ambegaokar, S. S., Ubeda, O. J., Frautschy, S. A., and Cole, G. M. (2004) Insulin-degrading enzyme as a downstream target of insulin receptor signaling cascade: implications for Alzheimer's disease intervention. *J. Neurosci.* **24,** 11120–11126
53. Hill, J. M., Lesniak, M. A., Pert, C. B., and Roth, J. (1986) Autoradiographic localization of insulin receptors in rat brain: prominence in olfactory and limbic areas. *Neuroscience* **17,** 1127–1138
54. Van Houten, M., and Posner, B. I. (1979) Insulin binds to brain blood vessels in vivo. *Nature* **282,** 623–625
55. Van Houten, M., and Posner, B. I. (1983) Circumventricular organs: receptors and mediators of direct peptide hormone action on brain. *Adv. Metab. Disord.* **10,** 269–289
56. Baskin, D. G., Davidson, D., Corp, E. S., Lewellen, T., and Graham, M. (1986) An inexpensive microcomputer digital imaging system for densitometry: quantitative autoradiography of insulin receptors with 125I and LKB ultrofilm. *J. Neurosci. Methods* **16,** 119–129
57. Unger, J., McNeill, T. H., Moxley, R. T., III, White, M., Moss, A., and Livingston, J. N. (1989) Distribution of insulin receptor-like immunoreactivity in the rat forebrain. *Neuroscience* **31,** 143–157
58. Werther, G. A., Hogg, A., Oldfield, B. J., McKinley, M. J., Figdor, R., Allen, A. M., and Mendelsohn, F. A. (1987) Localization and characterization of insulin receptors in rat brain and pituitary gland using in vitro autoradiography and computerized densitometry. *Endocrinology* **121,** 1562–1570
59. Schulingkamp, R. J., Pagano, T. C., Hung, D., and Raffa, R. B. (2000) Insulin receptors and insulin action in the brain: review and clinical implications. *Neurosci. Biobehav. Rev.* **24,** 855–872
60. Reger, M. A., Watson, G. S., Green, P. S., Wilkinson, C. W., Baker, L. D., Cholerton, B., Fishel, M. A., Plymate, S. R., Breitner, J. C., DeGroodt, W., Mehta, P., and Craft, S. (2008) Intranasal insulin improves cognition and modulates beta-amyloid in early AD. *Neurology* **70,** 440–448
61. Niedernhofer, L. J., Garinis, G. A., Raams, A., Lalai, A. S., Robinson, A. R., Appeldoorn, E., Odijk, H., Oostendorp, R., Ahmad, A., van Leeuwen, W., Theil, A. F., Vermeulen, W., van der Horst, G. T., Meinecke, P., Kleijer, W. J., Vijg, J., Jaspers, N. G., and Hoeijmakers, J. H. (2006) A new progeroid syndrome reveals that genotoxic stress suppresses the somatotroph axis. *Nature* **444,** 1038–1043

Received for publication March 16, 2009.
Accepted for publication May 7, 2009.

Journal of Gastroenterology and Hepatology JGHF

doi:10.1111/j.1440-1746.2009.06039.x

HEPATOLOGY

Adiponectin knockout mice on high fat diet develop fibrosing steatohepatitis

Takeharu Asano,* Kiyotaka Watanabe,* Naoto Kubota,† Toshiaki Gunji,* Masao Omata,* Takashi Kadowaki† and Shin Ohnishi*

*Department of Gastroenterology, †Department of Metabolic Disease, Graduate School of Medicine, University of Tokyo, Tokyo, Japan

Key words
adiponectin, animal model, high fat diet, liver fibrosis, non-alcoholic steatohepatitis.

Accepted for publication 8 February 2009.

Correspondence
Dr Shin Ohnishi, Department of Gastroenterology, Graduate School of Medicine, University of Tokyo, 7-3-1 Hongo, Bunkyo-ku, 113-8655 Tokyo, Japan. Email: sohnishi-tky@umin.ac.jp

Abstract

Background and Aim: Low levels of serum adiponectin have been reported to be associated with obesity, diabetes, and non-alcoholic steatohepatitis (NASH), as well as several malignancies. Adiponectin knockout (KO) mice have been reported to cause insulin resistance and neointimal formation of the artery. We used adiponectin KO mice fed a high fat (HF) diet, and investigated the effect of adiponectin on the progression of steatohepatitis and carcinogenesis *in vivo*.

Methods: Adiponectin KO mice and wild type (WT) mice were fed a HF diet or normal chow for the periods of 24 and 48 weeks. The HF diet contained 60% of calories from fat.

Results: The adiponectin KO mice on the HF diet showed obesity, marked elevation of serum transaminase levels, and hyperlipidemia. At 24 weeks, hepatic expression of tumor necrosis factor-α and procollagen α (I) was higher in KO mice as compared with WT mice. At 48 weeks, liver triglyceride contents in KO mice on normal chow were significantly higher than those in WT mice. Hepatocyte ballooning, spotty necrosis, and pericellular fibrosis around central veins were observed in KO mice on the HF diet. The pericellular fibrosis was more severe in KO mice on the HF diet than that in WT mice (1.62% *vs* 1.16%, $P = 0.033$). Liver adenoma and hyperplastic nodules developed in a KO mouse on the HF diet at 48 weeks (12.5%, $n = 1/8$), whereas no tumor was detected in WT mice ($n = 10$).

Conclusions: Adiponectin may play a protective role in the progression of NASH in the early stages by suppressing tumor necrosis factor-α expression and liver fibrosis.

Introduction

Non-alcoholic steatohepatitis (NASH) is thought to be a progressive disease and hepatic manifestation of the metabolic syndrome which includes insulin resistance, dyslipidemia, central obesity, and hypertension. NASH is the histological diagnosis characterized by macrovesicular steatosis, and includes inflammatory infiltration, ballooning hepatocyte, mallory's body, and varying degrees of fibrosis. A clinical study showed that about 20% of patients with NASH developed liver cirrhosis within 10 years,[1] and the cirrhotic stage of NASH appeared to be a high risk of hepatocellular carcinoma.[2,3] Moreover, steatosis accelerates the progression of fibrosis in chronic hepatitis C,[4,5] and reduces the likelihood of achieving early and sustained virologic response of interferon therapy.[6]

Adiponectin, a secreted protein derived from adipose tissue, has been reported to improve insulin resistance and hyperlipidemia,[7] and to reduce atherosclerosis.[8,9] Serum adiponectin levels are inversely correlated with body mass index of obese patients,[10] and are decreased in patients with type 2 diabetes and coronary artery disease.[11] Adiponectin increases glucose uptake and fatty acid oxidation in muscle, reduces glucose production in liver, and improves insulin sensitivity by activating adenosine 5′-monophosphate (AMP)-activated protein kinase[12] and peroxisome proliferator-activated receptor (PPAR) α.[13] Adiponectin attenuates liver fibrosis by suppressing the activity of hepatic stellate cells (HSCs) in a carbon tetrachloride-induced mouse model.[14] Tumor necrosis factor (TNF)-α is thought to be a causative factor of insulin resistance in obesity, and overexpression of TNF-α is found in the liver and in the adipose tissue of NASH patients.[15] Adiponectin inhibits TNF-α production in adipose tissue[16] as well as TNF-α-mediated activation of nuclear factor-κB signaling, and modulates the inflammatory response in vascular endothelial cells.[17]

Serum low adiponectin level has been reported to correlate with carcinogenesis of several malignancies including endometrial, breast, prostate, and colorectal cancers.[18] Regarding hepatocellular carcinoma, obesity[19] and diabetes[20] are reported to be risk factors of the cancer. High serum insulin level decreases mitochondrial β-oxidation of fatty acids, and induces inflammation and fibrosis. Adiponectin knockout (KO) mice treated with choline-deficient l-amino acid-defined diet developed liver cirrhosis and hepatic tumors.[21] Adiponectin appears to play an important role not only in the progression of NASH but also in NASH-related carcinogenesis.

There would be some differences between steatosis alone and steatohepatitis with oxidative stress and proinflammatory cytokines, and the role of adiponectin in each clinical stage has not been elucidated. To elucidate the pathophysiology of NASH, the analysis of several animal models including genetically modified models[22-26] and special diet models[27,28] has been reported. However, there is no animal model that accurately simulates the specific natural course and epidemiologic background of NASH in clinical situations.

In the present study, we used adiponectin KO mice fed a high fat (HF) diet for a long time, and investigated whether adiponectin has a physiological protective role against the progression of steatohepatitis and carcinogenesis *in vivo*.

Methods

Animals

In the present study, adiponectin KO mice have a C57Bl/6 × 129/sv genetic background. We previously reported that this animal model induced insulin resistance and glucose intolerance on normal chow, and caused neointimal formation of artery.[29] All mice used in the present study were male. Mice were provided the food and water ad libitum and were maintained on a 12 h light/dark cycle. Body weight of each mouse was measured every 2 weeks. Blood samples and liver tissues were collected from mice killed at 24 weeks (four mice per group), and 48 weeks (normal chow in WT [$n = 4$], KO [$n = 5$], and HF diet in WT [$n = 10$], KO [$n = 8$]). All animal care and experimental procedures conformed to the guidelines of the Animal Care Committee of the University of Tokyo.

High fat diet study

Mice were divided at random into two groups at 8 weeks of age. One group of mice was fed a HF diet (Nippon CLEA, Shizuoka, Japan) ad libitum, and the other was fed normal chow (Oriental Yeast, Suita, Japan). The HF diet contained 508 kcal/100 g, and 32% safflower oil, 33.1% casein, 17.6% sucrose, 5.6% cellulose. Calories from fat were 60% of total calories from the HF diet. Fatty acid of the HF diet consisted of saturated fatty acid 22% (palmitic acid 12.6%, stearic acid 8%) and unsaturated fatty acid 77% (oleic acid 64% and linoleic acid 10%). Normal chow contained 360 kcal/100 g, and 5.3% fat. Fat consisted of 13% of total calories on the HF diet. Calories per weight of HF diet were 1.4-fold those of normal chow.

Blood sample assay

Mice were fasted for > 16 h before blood sampling. Blood glucose levels were measured using an automatic blood glucose meter (Glutest Ace; Sanwa Chemical, Nagoya, Japan). Serum adiponectin levels were determined by mouse adiponectin enzyme-linked immunosorbent assay (ELISA) kit (Otsuka Pharmaceutical, Tokyo, Japan). Serum aspartate aminotransferase (AST), alanine aminotransferase (ALT), total cholesterol (TC), non-esterified fatty acid (NEFA), and triglyceride (TG) levels were determined by a transaminase CII-test, TC *E*-test, NEFA *C*-test, TG *E*-test (Wako Pure Chemical Industries, Osaka, Japan), respectively.

Liver TG content

Liver homogenates were extracted, and tissue triglyceride content was determined as described previously with an extract solution (chloroform : methanol = 2:1).[30]

Reverse transcription-polymerase chain reaction

Total RNA was prepared from liver tissue with TRIzol Reagent (Invitrogen, Carlsbad, CA, USA) according to the manufacturer's instructions. The RNA levels corresponding to various target genes were quantified using a polymerase chain reaction (PCR)-based technique. The extracted RNA was converted into cDNA by reverse transcription (TaqMan reverse transcription reagents, Applied Biosystems, Foster City, CA, USA). The cDNA solutions were analyzed by TaqMan technology, a real-time PCR assay (TaqMan PCR reagent kit, Applied Biosystems). Specific gene expression was quantified by real time PCR carried out on an ABI Prism 7900HT (Applied Biosystems). RNA expression of β-actin was measured as an internal control. Relative expression levels of target genes were compared after normalization to β-actin.

Histological analysis

Liver tissues were fixed with 10% formalin and embedded in paraffin. Cross-sections (5 μm thick) were cut and stained with hematoxylin and eosin (H&E). The extent of liver fibrosis was evaluated with Masson trichrome stain by the reported technique.[31,32] Areas around the central veins were chosen and quantitatively evaluated on sections stained with Masson trichrome for collagen. Thirty areas from a cross-section of each animal were digitized with a global magnification of ×200. Area calculations were based on measurements made with image editing (Photoshop, San Jose, CA, USA) and image analysis (Scion Image, Frederick, MD, USA) programs.

Statistical analysis

Results were expressed as mean ± standard deviation (SD). Differences of continuous data between groups were examined for statistical significance using Student's *t*-test (Stat View, Cary, NC, USA). Data were considered statistically significant at a $P < 0.05$.

Results

Mice on HF diet gradually gained weight

The appearance and body weight was similar between the wild type (WT) mice and the KO mice on the HF diet (Fig. 1a). On the HF diet, body weights in both mice groups were significantly heavier than those on normal chow, and increased from 24 to 48 weeks (Fig. 1b).

Effect of HF diet on serum adiponectin levels

The serum adiponectin levels in WT mice on the HF diet tended to decrease (65%) from 24 to 48 weeks ($P = 0.097$), whereas mice on normal chow showed very small interval change (Fig. 2a). The serum adiponectin levels of KO mice were below detection limits.

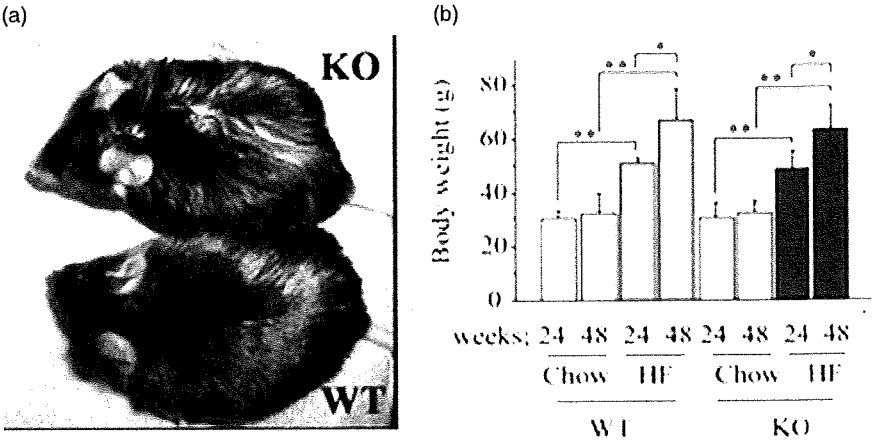

Figure 1 Mice on the high fat (HF) diet showed obesity. (a) The photograph shows wild type (WT) mice and knockout (KO) mice on the HF diet at 48 weeks. The appearances were similar between WT and adiponectin KO mice. (b) Body weights are shown at 24 and 48 weeks in WT and adiponectin KO mice. Each value is mean ± standard deviation (SD), significance at $*P < 0.05$, $**P < 0.01$.

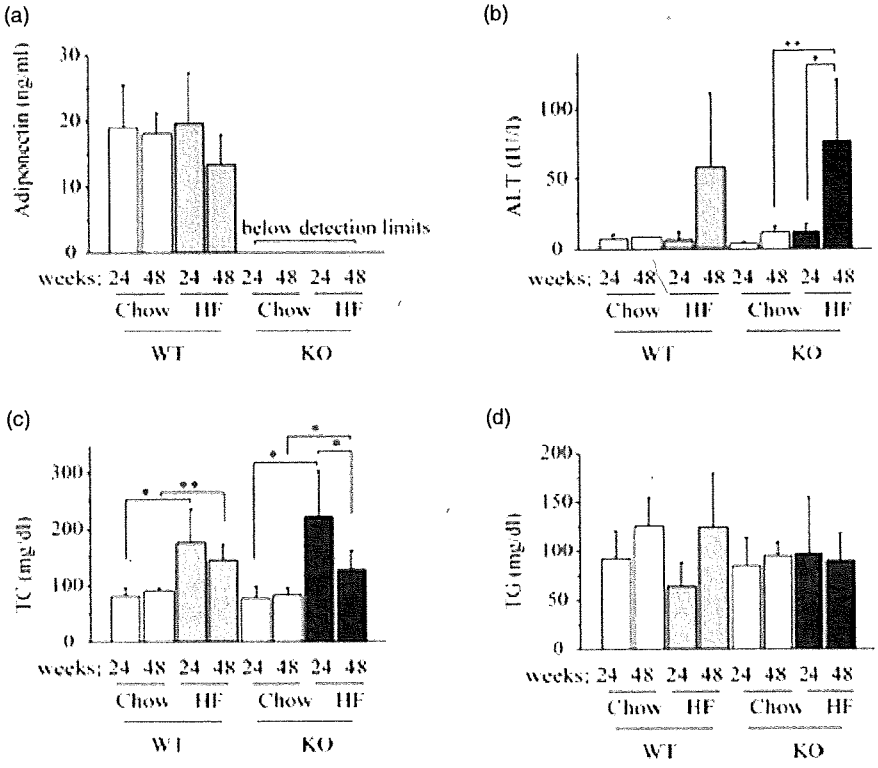

Figure 2 Mice on the high fat (HF) diet showed hyperglycemia, hyperlipidemia, and transaminase elevation. Serum levels of (a) adiponectin, (b) alanine aminotransferase (ALT), (c) total cholesterol (TC), and (d) triglyceride (TG) were measured in wild type (WT) and adiponectin knockout (KO) mice at 24 and 48 weeks. Each value is mean ± standard deviation (SD), significance at $*P < 0.05$, $**P < 0.01$.

Serum transaminase and lipid levels in adiponectin KO mice

The blood glucose levels in both WT and KO mice on the HF diet were significantly higher than that of mice on normal chow (data not shown). Serum ALT levels in KO mice on the HF diet were significantly higher than that of mice on normal chow at 48 weeks (Fig. 2b), and AST levels were similar. Serum TC levels were significantly higher in both WT and KO mice on the HF diet than that of mice on normal chow at 24 weeks (Fig. 2c). Serum TG levels in WT mice tended to increase from 24 to 48 weeks (Fig. 2d). Serum NEFA (data not shown), TC, TG levels were similar between WT and KO mice.

Liver TG contents in adiponectin KO mice

The liver of mice on the HF diet was enlarged and homogeneously white in color (Fig. 3a). The liver TG contents in KO mice on normal chow were significantly higher than that of WT mice at 48 weeks, although there was no significant difference between WT and KO mice on the HF diet (Fig. 3b).

Hepatic RNA expression of TNF-α was significantly higher in adiponectin KO mice

At 24 weeks, hepatic RNA expression of TNF-α in KO mice on the HF diet was significantly higher by threefold than that in WT mice

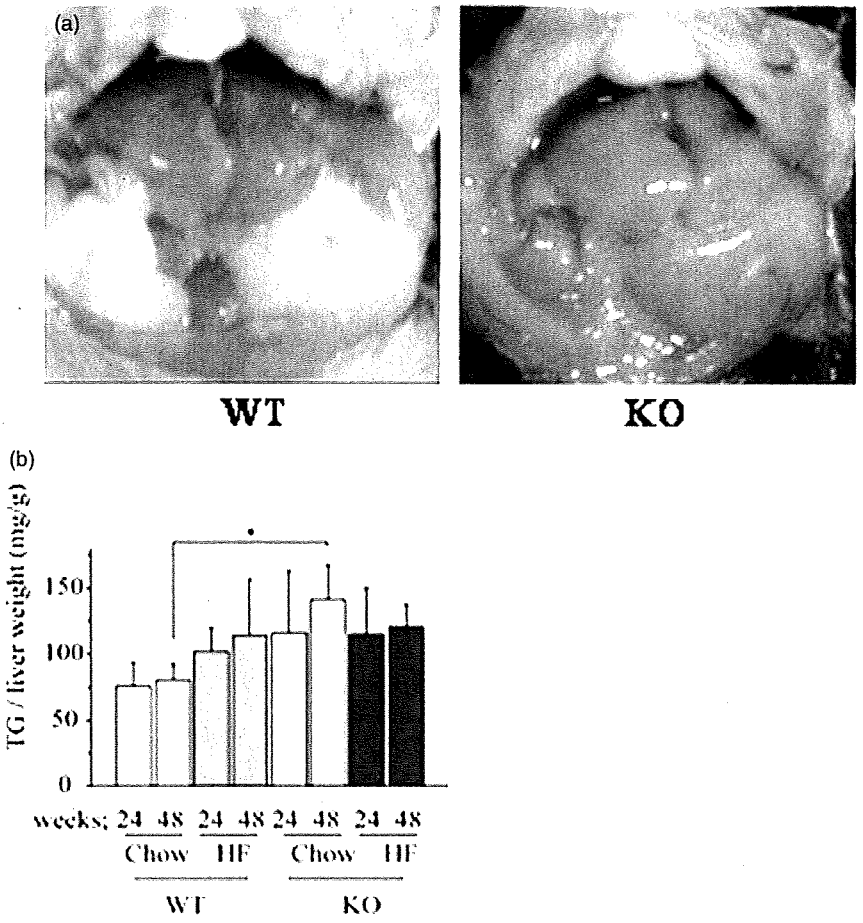

Figure 3 Liver triglyceride (TG) contents in Adiponectin knockout (KO) mice on normal chow were significantly higher as compared with wild type (WT) mice. (a) The photograph shows livers of WT mice and adiponectin KO mice on the high fat (HF) diet at 48 weeks. The appearances of liver were similar between WT and KO mice. (b) The liver TG contents were measured in WT and adiponectin KO mice at 24 and 48 weeks. Each value is the mean ± standard deviation (SD), significance at $^{*}P < 0.05$, $^{**}P < 0.01$.

($P = 0.03$) (Fig. 4a). The expression of procollagen α (I) in KO mice on the HF diet was higher by fourfold than that in WT mice at 24 weeks (Fig. 4b). The expression of lipogenic genes such as Sterol Regulatory Element-binding Protein (SREBP)-1c, stearoyl Co-A desaturase-1 (SCD1) was significantly higher on the HF diet in both WT and KO mice than that in mice on normal chow (data not shown). The expression of cyclin D1 in KO mice on the HF diet was significantly higher than that in mice on normal chow, and it tended to be higher by 1.5-fold that in WT mice at 48 weeks (Fig. 4c).

Adiponectin KO mice showed steatohepatitis with pericellular fibrosis

In histopathological analysis of mice on normal chow, hepatic tissue appeared almost normal at 24 weeks and 48 weeks in WT mice, and at 24 weeks in KO mice. Some KO mice on normal chow at 48 weeks showed mild lipid accumulation around central veins. The liver of WT and KO mice on HF diet showed massive hepatocyte ballooning around central veins, but almost no fibrosis was detected by Masson trichrome staining (Fig. 5a). At 48 weeks, KO mice showed lobular lipid accumulation, prominent hepatocyte ballooning, spotty necrosis, Mallory body, eosinophilic focus, and notable pericellular fibrosis (Fig. 5b). According to human NASH criteria reported by Brunt *et al.* these features were matched to Grade 3, Stage 1. Hepatic fibrosis areas around central veins were quantitatively evaluated, and the fibrosis in KO mice was more severe than that in WT mice at 48 weeks (1.16 ± 0.4% *vs* 1.62 ± 0.43%, respectively, $P = 0.033$) (Fig. 5c).

Adenoma developed in the liver of an adiponectin KO mouse at 48 weeks

A liver tumor of 10 mm in diameter was detected in one of the KO mice (12.5%, $n = 1/8$) at 48 weeks (Fig. 6a). The tumor contained a large fat deposit with mild atypia, and was diagnosed as liver adenoma (Fig. 6b,c). Histology of other small nodular lesions that were detected in the same mouse was regenerative hyperplastic alteration. In contrast, no tumor was detected in the livers of WT mice ($n = 10$).

Discussion

In the present study, adiponectin KO mice on the HF diet showed steatosis, inflammation, fibrosis, and tumor formation, which are well recognized as pathological features specific for NASH. The mice had taken the HF diet that did not contain chemicals promoting liver fibrosis such as endotoxin or carbon tetrachloride, and thus are considered to be an animal model of NASH.

Several animal models of NASH have been advocated to date. Methionine-choline deficient diet and the choline-deficient L-amino acid-defined diet model showed steatosis, liver fibrosis, and liver tumors, without obesity.[28] Mice fed the HF liquid diet by

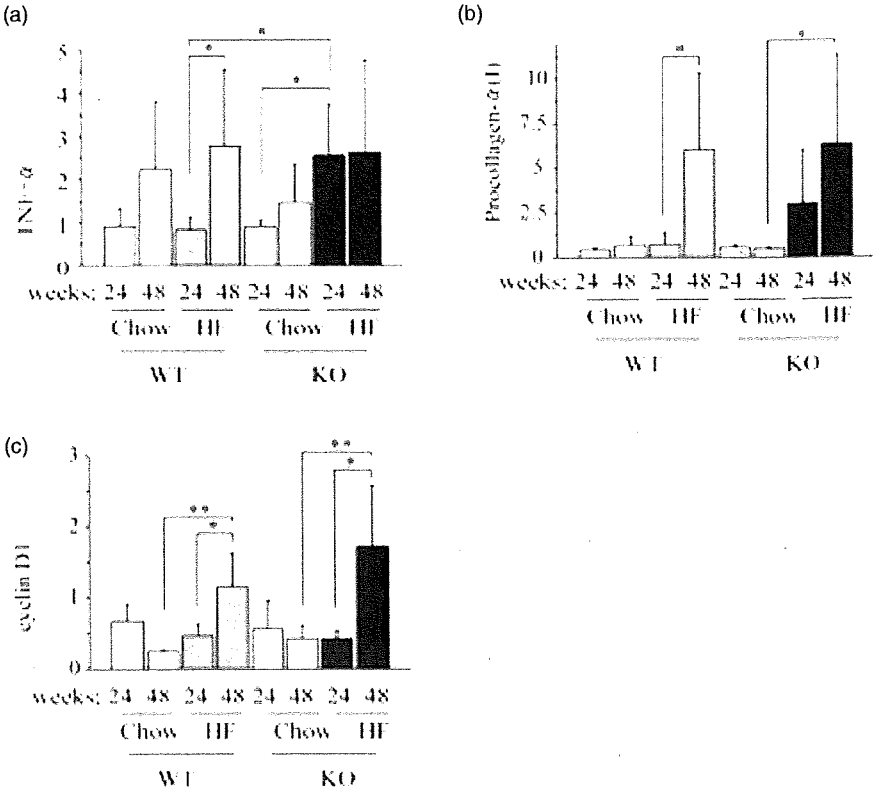

Figure 4 Hepatic expression of tumor necrosis factor-α (TNF-α) was significantly higher in adiponectin knockout (KO) mice. Hepatic RNA expression levels of (a) TNF-α, (b) procollagen α (I), and (c) cyclin D1 were measured in wild type (WT) and adiponectin KO mice at 24 and 48 weeks. Each value is mean ± standard deviation (SD), significance at $*P < 0.05$, $**P < 0.01$.

implanted gastrostomy tube induced NASH without liver tumor.[27] Liver-specific PTEN KO mice showed macrovesicular steatosis, liver fibrosis, and tumors.[26] However, there has been no report of mouse model developing NASH on a HF diet alone. HF composition is epidemiologically considered one of the main causes of obesity and NASH. Clinical study in humans requires a lengthy amount of time to estimate fibrosis or progression in the natural course of NASH. Therefore, we used the animal model and estimated outcomes during the limited period. We chose adiponectin KO mice because NASH is commonly associated with hypoadiponectinemia in humans.[33] We hope this model will provide beneficial clues to clinical studies of diet therapy or drug development for obesity and steatohepatitis.

Some of the KO mice on normal chow at 48 weeks showed mild lipid accumulation around the central veins, and the liver TG contents were significantly higher than that of WT mice. KO mice were susceptible to liver TG accumulation on normal chow. However, there was no significant difference of liver TG contents between KO mice and WT mice on the HF diet. There might be a limit of liver TG accumulation volume for a certain period. These features might resemble the state of 'burned-out' NASH in which the lipid accumulation and inflammation become unremarkable in the progressed NASH patient.[34]

Hepatic expression of TNF-α was significantly higher in adiponectin KO mice on the HF diet at 24 weeks (early stage), and maintained a high level until 48 weeks (late fibrotic stage). TNF-α induces insulin resistance by inhibiting the tyrosine phosphorylation of insulin receptor substance-1,[35] and would lead to a vicious circle of escalating steatosis. On the other hand, TNF-α has functions of inducing apoptosis, and attenuating the resistance against necrosis. Adiponectin KO mice on a HF diet at 48 weeks showed hepatic spotty necrosis and Mallory body, which indicated liver injury. Adiponectin inhibits TNF-α production in adipose tissue[16] and TNF-α-mediated activation of nuclear factor-κB signaling through a cAMP-dependent pathway.[17] In the liver, the majority of TNF-α is produced by Kupffer cells. Alcoholic steatohepatitis has been reported to enhance Kupffer cells sensitization to endotoxin (lipopolysaccharide), and increase TNF-α production.[36] Also in NASH patients, it is hypothesized that the liver might be highly susceptible to adipocytokines from intraperitoneal massive adipose tissue and endotoxine from the intestinal tract.

The expression of procollagen α (I) as well as TNF-α was higher at 24 weeks, and subsequent hepatic fibrosis was significantly promoted at 48 weeks in adiponectin KO mice on the HF diet as compared with the WT mice. TNF-α induces activation of HSC directly and stimulates production of transforming growth factor (TGF)-β. HSC plays central roles in liver fibrosis with TGF-β and collagens.[37] TGF-β is a main mediator of proliferation and migration for HSC, and activated HSC enhances the expression of procollagen α, which is the target gene of TGF-β. Thus, adiponectin might suppress not only TNF-α mediated inflammation, but also TNF-α-induced liver fibrosis. Elevation of TNF-α in the early stage may indicate HSC activation and fibrosis at a late stage. At 48 weeks, serum adiponectin in WT mice tended to be decreased, so the difference in TNF-α and procollagen might be little between WT and KO mice. Kamada *et al.* reported that the carbon tetrachloride administered adiponectin KO mice showed extensive liver fibrosis with activation of HSC and overexpression of TGF-β1. Notably, the fibrosis was improved by supplementation of

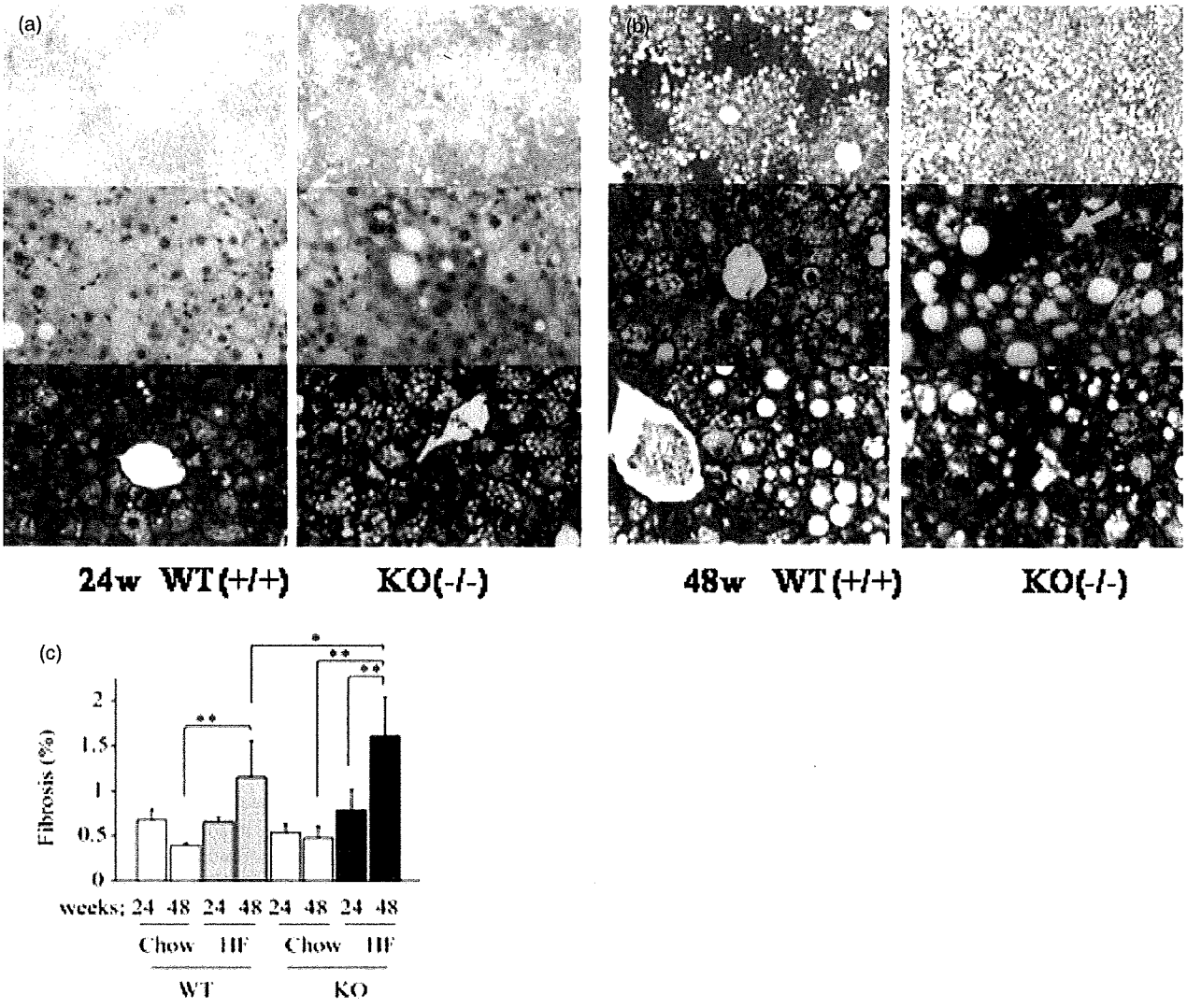

Figure 5 Adiponectin knockout (KO) mice showed steatohepatitis. (a) The liver sections of wild type (WT) and adiponectin KO mice on the high fat (HF) diet at 24 weeks. The first and second rows show a lower (×40) and higher (×200) magnification of hematoxylin and eosin (H&E)-stained livers, respectively. Hepatocyte ballooning was observed around central veins. Liver fibrosis was not detected by Masson trichrome staining in either model (third row, magnifications ×200). (b) The liver sections of WT and adiponectin KO mice on the HF diet at 48 weeks. The first and second rows show a lower (×40) and higher (×200) magnification of H&E-stained livers, respectively. Adiponectin KO mice showed lobular lipid accumulation, hepatocyte ballooning, spotty necrosis (arrow) and especially pericellular fibrosis around the central veins as determined by Masson trichrome staining (third row, magnifications ×200). (c) Hepatic fibrosis areas around the central veins were measured in WT and adiponectin KO mice at 24 and 48 weeks. Each value is mean ± standard deviation (SD), significance at $*P < 0.05$, $**P < 0.01$.

adiponectin.[14] Thus, adiponectin is considered to play a protective role against liver fibrosis by suppressing TNF-α expression.

Peroxisome proliferator-activated receptor γ is primarily localized to HSC, and PPARγ agonist inhibits proliferation and activation of human HSC.[38] Evidence of improvement to NASH was demonstrated by use of PPARγ agonist. PPARγ agonist improved insulin resistance and histological features including fibrosis.[39] The action of PPARγ agonist has been reported to occur with adiponectin dependently in the liver and adiponectin independently in skeletal muscle.[40]

A liver adenoma was detected in one of the adiponectin KO mice on the HF diet at 48 weeks, though any tumor was not detected in WT mice. In the present study, KO mice have a C57Bl/6 × 129/sv genetic background that rarely develops into liver tumor.[41] CDAA diet in adiponectin KO mice was reported to accelerate liver tumor formation.[21] Recently, it has been more frequently reported that hepatocellular carcinoma in patients with cryptogenic cirrhosis might be associated with NASH.[2,42] Larger prospective clinical studies of patients with NASH are needed to establish the risk of carcinogenesis.

Hepatic expression of cyclin D1 was higher in adiponectin KO mice on the HF diet at 48 weeks. Cyclin D1 is thought to play a critical role in transition from the G1 to S Phase of the cell cycle. The overexpression of cyclin D1 can provoke a perturbed

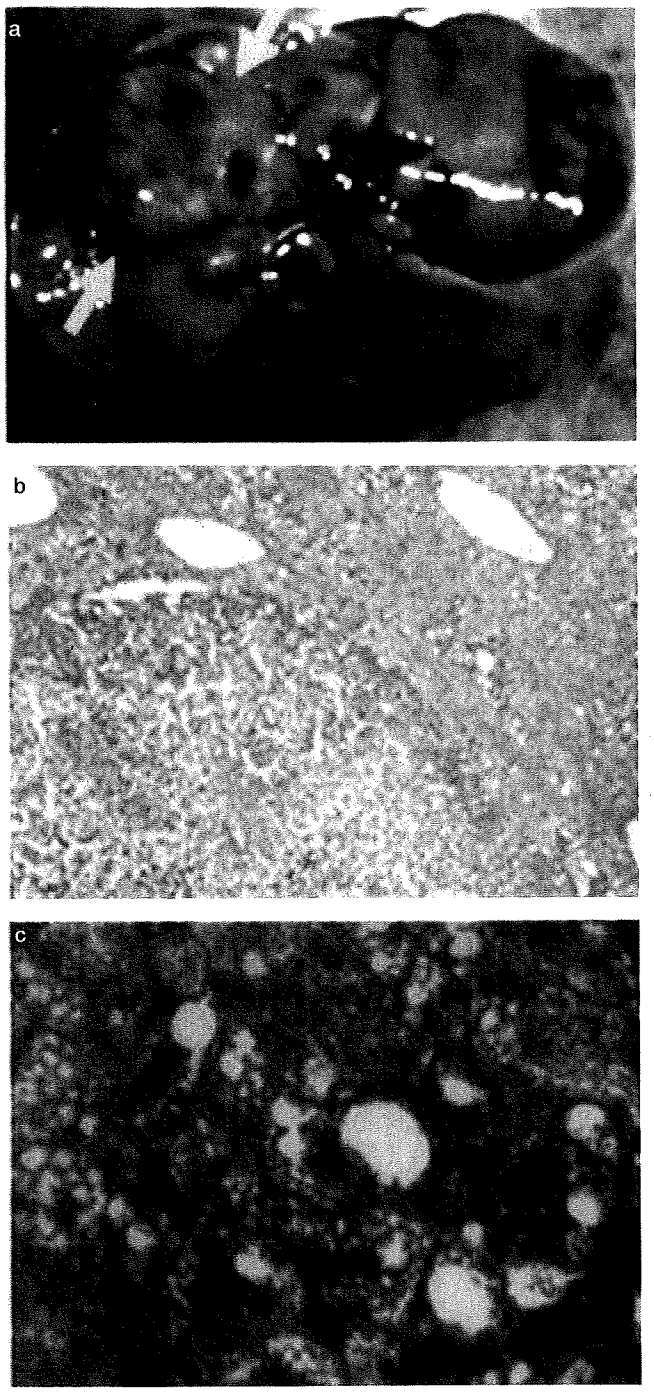

Figure 6 Liver adenoma was observed in an adiponectin knockout (KO) mouse. (a) A liver tumor of 10 mm in diameter was observed (arrow) in one of the adiponectin KO mice (12.5%, $n = 1/8$) at 48 weeks. The tumor had grown pressing surrounded normal liver architecture and partially protruding from the liver. (b) Hematoxylin and eosin (H&E)-stained section of the liver tumor in (a). The tumor hepatocytes contained large amounts of fat deposits. The border between the tumor and surrounding normal liver parenchyma is clear. (c) H&E-stained section of the liver tumor with mild atypia, diagnosed as adenoma. Magnifications are ×40 (b), ×200 (c).

progression of the G1 phase of the cell cycle. Rearrangement, amplification, and overexpression of the cyclin D1 gene have been detected in several types of cancers, including esophageal, breast, and liver cancers.[43,44] Microvesicular steatosis and hepatocellular carcinoma with overexpression of cyclin D1 was observed in retinoic acid receptor-α dominant negative form transgenic mouse, and the carcinogenesis was considered to be caused by Wnt signal activation with loss of retinoic acid signal.[25] Hepatic steatosis is frequently observed in hepatitis C virus (HCV)-infected patients. Analysis of HCV core gene transgenic mice suggested that hepatocarcinogenesis in HCV infection may be associated with mitochondrial dysfunction, reactive oxygen species overproduction,[45] enhanced expression of TNF-α, activation of activator protein-1,[46] and activation of retinoic acid receptor-α.[47] The mechanism of carcinogenesis in NASH still remains uncertain. Therefore, experimental study in the NASH model would require a further examination including genetic analysis.

In conclusion, adiponectin KO mice on a HF diet for a prolonged period induced obesity, hyperlipidemia, steatohepatitis, pericellular fibrosis, and adenoma formation. These mice showed natural history and features very similar to the pathogenesis of NASH in human. Adiponectin may play a protective role against the progression of NASH in the early stage by suppression of TNF-α expression and liver fibrosis. Deficiency of adiponectin may participate in liver carcinogenesis related to steatohepatitis.

Acknowledgments

The present study was supported by the Program of Fundamental Studies in Health Sciences of the National Institute of Biomedical Innovation (NIBIO), by the NFAT project of New Energy and Industrial Technology Development Organization (NEDO) and by the Special Coordination Fund for Science and Technology from the Ministry of Education, Culture, Sports, Science and Technology, Japan.

References

1 Matteoni CA, Younossi ZM, Gramlich T, Boparai N, Liu YC, McCullough AJ. Nonalcoholic fatty liver disease: a spectrum of clinical and pathological severity. *Gastroenterology* 1999; **116**: 1413–9.
2 Bugianesi E, Leone N, Vanni E *et al.* Expanding the natural history of nonalcoholic steatohepatitis: from cryptogenic cirrhosis to hepatocellular carcinoma. *Gastroenterology* 2002; **123**: 134–40.
3 Marrero JA, Fontana RJ, Su GL, Conjeevaram HS, Emick DM, Lok AS. NAFLD may be a common underlying liver disease in patients with hepatocellular carcinoma in the United States. *Hepatology* 2002; **36**: 1349–54.
4 Hourigan LF, Macdonald GA, Purdie D *et al.* Fibrosis in chronic hepatitis C correlates significantly with body mass index and steatosis. *Hepatology* 1999; **29**: 1215–19.
5 Adinolfi LE, Gambardella M, Andreana A, Tripodi MF, Utili R, Ruggiero G. Steatosis accelerates the progression of liver damage of chronic hepatitis C patients and correlates with specific HCV genotype and visceral obesity. *Hepatology* 2001; **33**: 1358–64.
6 Patton HM, Patel K, Behling C *et al.* The impact of steatosis on disease progression and early and sustained treatment response in chronic hepatitis C patients. *J. Hepatol.* 2004; **40**: 484–90.

7 Yamauchi T, Kamon J, Minokoshi Y *et al.* Adiponectin stimulates glucose utilization and fatty-acid oxidation by activating AMP-activated protein kinase. *Nat. Med.* 2002; **8**: 1288–95.
8 Matsuda M, Shimomura I, Sata M *et al.* Role of adiponectin in preventing vascular stenosis. The missing link of adipo-vascular axis. *J. Biol. Chem.* 2002; **277**: 37 487–91.
9 Okamoto Y, Kihara S, Ouchi N *et al.* Adiponectin reduces atherosclerosis in apolipoprotein E-deficient mice. *Circulation* 2002; **106**: 2767–70.
10 Arita Y, Kihara S, Ouchi N *et al.* Paradoxical decrease of an adipose-specific protein, adiponectin, in obesity. *Biochem. Biophys. Res. Commun.* 1999; **257**: 79–83.
11 Hotta K, Funahashi T, Arita Y *et al.* Plasma concentrations of a novel, adipose-specific protein, adiponectin, in type 2 diabetic patients. *Arterioscler. Thromb. Vasc. Biol.* 2000; **20**: 1595–9.
12 Yamauchi T, Kamon J, Waki H *et al.* The fat-derived hormone adiponectin reverses insulin resistance associated with both lipoatrophy and obesity. *Nat. Med.* 2001; **7**: 941–6.
13 Yamauchi T, Kamon J, Waki H *et al.* Globular adiponectin protected ob/ob mice from diabetes and ApoE-deficient mice from atherosclerosis. *J. Biol. Chem.* 2003; **278**: 2461–8.
14 Kamada Y, Tamura S, Kiso S *et al.* Enhanced carbon tetrachloride-induced liver fibrosis in mice lacking adiponectin. *Gastroenterology* 2003; **125**: 1796–807.
15 Crespo J, Cayon A, Fernandez Gil P *et al.* Gene expression of tumor necrosis factor alpha and TNF-receptors, p55 and p75, in nonalcoholic steatohepatitis patients. *Hepatology* 2001; **34**: 1158–63.
16 Maeda N, Shimomura I, Kishida K *et al.* Diet-induced insulin resistance in mice lacking adiponectin/ACRP30. *Nat. Med.* 2002; **8**: 731–7.
17 Ouchi N, Kihara S, Arita Y *et al.* Adiponectin, an adipocyte-derived plasma protein, inhibits endothelial NF-kappaB signaling through a cAMP-dependent pathway. *Circulation* 2000; **102**: 1296–301.
18 Kelesidis I, Kelesidis T, Mantzoros CS. Adiponectin and cancer: a systematic review. *Br. J. Cancer* 2006; **94**: 1221–5.
19 Calle EE, Rodriguez C, Walker Thurmond K, Thun MJ. Overweight, obesity, and mortality from cancer in a prospectively studied cohort of U.S. adults. *N. Engl. J. Med.* 2003; **348**: 1625–38.
20 El Serag HB, Tran T, Everhart JE. Diabetes increases the risk of chronic liver disease and hepatocellular carcinoma. *Gastroenterology* 2004; **126**: 460–8.
21 Kamada Y, Matsumoto H, Tamura S *et al.* Hypoadiponectinemia accelerates hepatic tumor formation in a nonalcoholic steatohepatitis mouse model. *J. Hepatol.* 2007; **47**: 556–64.
22 Fan CY, Pan J, Usuda N, Yeldandi AV, Rao MS, Reddy JK. Steatohepatitis, spontaneous peroxisome proliferation and liver tumors in mice lacking peroxisomal fatty acyl-CoA oxidase. Implications for peroxisome proliferator-activated receptor alpha natural ligand metabolism. *J. Biol. Chem.* 1998; **273**: 15639–45.
23 Lu SC, Alvarez L, Huang ZZ *et al.* Methionine adenosyltransferase 1A knockout mice are predisposed to liver injury and exhibit increased expression of genes involved in proliferation. *Proc. Natl Acad. Sci. USA* 2001; **98**: 5560–5.
24 Martinez Chantar ML, Corrales FJ, Martinez Cruz LA *et al.* Spontaneous oxidative stress and liver tumors in mice lacking methionine adenosyltransferase 1A. *FASEB J.* 2002; **16**: 1292–4.
25 Yanagitani A, Yamada S, Yasui S *et al.* Retinoic acid receptor alpha dominant negative form causes steatohepatitis and liver tumors in transgenic mice. *Hepatology* 2004; **40**: 366–75.
26 Horie Y, Suzuki A, Kataoka E *et al.* Hepatocyte-specific Pten deficiency results in steatohepatitis and hepatocellular carcinomas. *J. Clin. Invest.* 2004; **113**: 1774–83.
27 Deng QG, She H, Cheng JH *et al.* Steatohepatitis induced by intragastric overfeeding in mice. *Hepatology* 2005; **42**: 905–14.
28 Koteish A, Diehl AM. Animal models of steatosis. *Semin. Liver Dis.* 2001; **21**: 89–104.
29 Kubota N, Terauchi Y, Yamauchi T *et al.* Disruption of adiponectin causes insulin resistance and neointimal formation. *J. Biol. Chem.* 2002; **277**: 25863–6.
30 Murakami K, Tobe K, Ide T *et al.* A novel insulin sensitizer acts as a coligand for peroxisome proliferator-activated receptor-alpha (PPAR-alpha) and PPAR-gamma: effect of PPAR-alpha activation on abnormal lipid metabolism in liver of Zucker fatty rats. *Diabetes* 1998; **47**: 1841–7.
31 Caballero T, Perez Milena A, Masseroli M *et al.* Liver fibrosis assessment with semiquantitative indexes and image analysis quantification in sustained-responder and non-responder interferon-treated patients with chronic hepatitis C. *J. Hepatol.* 2001; **34**: 740–7.
32 Ikura Y, Ohsawa M, Shirai N *et al.* Expression of angiotensin II type 1 receptor in human cirrhotic livers: Its relation to fibrosis and portal hypertension. *Hepatol. Res.* 2005; **32**: 107–16.
33 Hui JM, Hodge A, Farrell GC, Kench JG, Kriketos A, George J. Beyond insulin resistance in NASH: TNF-alpha or adiponectin? *Hepatology* 2004; **40**: 46–54.
34 Caldwell SH, Oelsner DH, Iezzoni JC, Hespenheide EE, Battle EH, Driscoll CJ. Cryptogenic cirrhosis: clinical characterization and risk factors for underlying disease. *Hepatology* 1999; **29**: 664–9.
35 Hotamisligil GS, Spiegelman BM. Tumor necrosis factor alpha: a key component of the obesity-diabetes link. *Diabetes* 1994; **43**: 1271–8.
36 Enomoto N, Takei Y, Hirose M *et al.* Thalidomide prevents alcoholic liver injury in rats through suppression of Kupffer cell sensitization and TNF-alpha production. *Gastroenterology* 2002; **123**: 291–300.
37 Friedman SL. Seminars in medicine of the Beth Israel Hospital, Boston. The cellular basis of hepatic fibrosis. Mechanisms and treatment strategies. *N. Engl. J. Med.* 1993; **328**: 1828–35.
38 Galli A, Crabb D, Price D *et al.* Peroxisome proliferator-activated receptor gamma transcriptional regulation is involved in platelet-derived growth factor-induced proliferation of human hepatic stellate cells. *Hepatology* 2000; **31**: 101–8.
39 Promrat K, Lutchman G, Uwaifo GI *et al.* A pilot study of pioglitazone treatment for nonalcoholic steatohepatitis. *Hepatology* 2004; **39**: 188–96.
40 Kubota N, Terauchi Y, Kubota T *et al.* Pioglitazone ameliorates insulin resistance and diabetes by both adiponectin-dependent and -independent pathways. *J. Biol. Chem.* 2006; **281**: 8748–55.
41 Stevens LC, Little CC. Spontaneous testicular teratomas in an inbred strain of Mice. *Proc. Natl Acad. Sci. USA* 1954; **40**: 1080–7.
42 Ratziu V, Bonyhay L, Di Martino V *et al.* Survival, liver failure, and hepatocellular carcinoma in obesity-related cryptogenic cirrhosis. *Hepatology* 2002; **35**: 1485–93.
43 Hunter T, Pines J. Cyclins and cancer. II: Cyclin D and CDK inhibitors come of age. *Cell* 1994; **79**: 573–82.
44 Zhang YJ, Jiang W, Chen CJ *et al.* Amplification and overexpression of cyclin D1 in human hepatocellular carcinoma. *Biochem. Biophys. Res. Commun.* 1993; **196**: 1010–16.
45 Moriya K, Nakagawa K, Santa T *et al.* Oxidative stress in the absence of inflammation in a mouse model for hepatitis C virus-associated hepatocarcinogenesis. *Cancer Res.* 2001; **61**: 4365–70.
46 Tsutsumi T, Suzuki T, Moriya K *et al.* Alteration of intrahepatic cytokine expression and AP-1 activation in transgenic mice expressing hepatitis C virus core protein. *Virology* 2002; **304**: 415–24.
47 Tsutsumi T, Suzuki T, Shimoike T *et al.* Interaction of hepatitis C virus core protein with retinoid X receptor alpha modulates its transcriptional activity. *Hepatology* 2002; **35**: 937–46.

Protective effects of citrus nobiletin and auraptene in transgenic rats developing adenocarcinoma of the prostate (TRAP) and human prostate carcinoma cells

MingXi Tang,[1] Kumiko Ogawa,[1,3] Makoto Asamoto,[1] Naomi Hokaiwado,[1] Azman Seeni,[1] Shugo Suzuki,[1] Satoru Takahashi,[1] Takuji Tanaka,[2] Kazuhito Ichikawa[1] and Tomoyuki Shirai[1]

[1]Department of Experimental Pathology and Tumor Biology, Nagoya City University Graduate School of Medical Sciences, 1 Kawasumi, Mizuho-cho, Mizuho-ku, Nagoya 467-8601; [2]Department of Oncologic Pathology, Kanazawa Medical University, 1-1 Daigaku, Uchinada, Ishikawa 920-0293, Japan

(Received October 13, 2006/Revised December 5, 2006/Accepted December 10, 2006/Online publication January 26, 2007)

Dietary phytochemicals, including nobiletin and auraptene, have been shown to exert inhibiting effects in several chemically induced carcinogenesis models. We here investigated the influence of nobiletin and auraptene on prostate carcinogenesis using transgenic rats developing adenocarcinoma of the prostate (TRAP) bearing the SV40 T antigen transgene under control of the probasin promoter and human prostate cancer cells. Starting at 5 weeks of age, male TRAP rats received powder diet containing 500 p.p.m. nobiletin or auraptene, or the basal diet for 15 weeks and then were sacrificed for analysis of serum testosterone levels and histological changes. The body and relative prostate weights and serum testosterone levels did not differ among the groups. Since all animals developed prostate carcinomas, these were semiquantitatively measured and expressed as relative areas of prostate epithelial cells. Nobiletin caused significant reduction in the ventral ($P < 0.01$), lateral ($P < 0.001$) and dorsal ($P < 0.05$) prostate lobes, while decreasing high grade lesions ($P < 0.05$) in the ventral and lateral lobes. Feeding of auraptene also effectively reduced the epithelial component ($P < 0.05$) and high grade lesions ($P < 0.05$), in the lateral prostate. A further experiment demonstrated that growth of androgen sensitive LNCaP and androgen insensitive DU145 and PC3 human prostate cancer cells, was suppressed by both nobiletin and to a lesser extent auraptene in a dose-dependent manner, with significant increase in apoptosis. In conclusion, these compounds, particularly nobiletin, may be valuable for prostate cancer prevention. (*Cancer Sci* 2007; 98: 471–477)

Prostate cancer is the most common malignant disease overall in the US and western countries and the second leading cause of cancer-related deaths among men.[1] It has been estimated that 234 460 new cases of prostate cancer will be diagnosed and that 27 350 deaths related to prostate cancer will occur in the US alone in 2006.[1] There are potentially curative options such as radical prostatectomy or radiotherapy, but once the disease is metastatic, the outlook is poor. Therefore chemoprevention or chemical control of prostate cancer has become an important priority. Since the intake of citrus fruits has been found to be beneficial for cancer prevention by epidemiological survey,[2] we here focused attention on nobiletin (5,6,7,8,3′,4′-hexamethoxyflavone), a polymethoxy-flavonoid extracted from citrus fruits such as oranges.[3] It has been shown to exert antibacterial,[4] anti-inflammatory,[5,6] antimutagenic,[7] antioxidative[6] and antitumor initiation[8] effects, while also inhibiting proliferation of human squamous cancer cells,[9] and hepatocarcinoma cells,[10] and suppressing the production of matrix metalloproteinase-1, -7 and -9.[11–13] *In vivo* studies have demonstrated that nobiletin inhibits peritoneal dissemination of gastric cancer in severe combined immunodeficiency (SCID) mice,[14] as well as azoxymethane (AOM)-induced large bowel carcinogenesis.[15] Thus this chemical appears to be a promising agent for suppression of cancer cell induction, invasion and metastasis.

Auraptene, a prenyloxycoumarin antioxidant agent also isolated from the citrus fruits such as natsumikans or grapefruit,[16,17] has similarly been found to exert preventive potential, suppressing 12-0-tetradecanoylphorbol-13-acetate (TPA)-induced tumor promotion in mouse skin,[16] and chemically induced carcinogenesis in large bowel,[18] oral cavity,[19] esophagus,[20] and liver[21,22] in rats. Recently, it was reported that dietary administration of auraptene inhibits colitis-related colon carcinogenesis,[23] and lung metastasis of melanoma cells in mice.[24]

We hypothesized that citrus nobiletin or auraptene may afford chemopreventive effects against prostate cancer in *in vivo* and *in vitro*, and therefore investigated their influence on the transgenic rats developing adenocarcinoma of the prostate (TRAP) model which was generated in our laboratory and features well-differentiated prostate adenocarcinomas in all prostatic lobes in a short period (15 weeks of age).[25–29] The TRAP rat has a transgene which encodes SV40/Tag under probasin promoter, so that the developed carcinomas are androgen-dependent. Furthermore, we examined chemotherapeutic effects and possible mechanisms using human prostate cancer cells *in vitro*.

Materials and Methods

Animals and chemicals. TRAP rats for the experiment were obtained by mating heterologous males, established in our laboratory with a Sprague-Dawley (SD) genetic background,[25,30] with wild-type female SD rats (Clea, Tokyo, Japan). The hybrid litters were screened by PCR, as described previously,[29] and male transgenic rats were selected for use in the experiment. All animals were housed 3/plastic cage on wood-chip bedding in an air-conditioned specific pathogen-free (SPF) animal room at 22 ± 2°C and 55 ± 5% humidity with a 12 h light/dark cycle and fed powdered basal diet (Oriental MF, Oriental Yeast Co., Tokyo, Japan), with or without chemical supplements, and water *ad libitum*. All animal experiments were performed under protocols approved by the Institutional Animal Care and Use Committee of Nagoya City University School of Medical Sciences. Nobiletin (> 98% purity; lot no. 050621) and auraptene (>98% purity; lot no. 040220) were purchased from Nard Chemicals Co., Ltd. (Amagasaki, Hyogo, Japan). The doses of the test compounds for the animal experiments were selected based on previous chemopreventive studies.[18]

Animal experimental protocols, blood collection and tissue sampling. Starting at 5 weeks of age, 27 rats in three groups (9 rats per group) received powder diet containing 500 p.p.m.

[3]To whom correspondence should be addressed. E-mail: kogawa@med.nagoya-cu.ac.jp

doi: 10.1111/j.1349-7006.2007.00417.x